CONFIDENTIAL [redacted]

OFFICE OF SCIENTIFIC RESEARCH & DEVELOPMENT
NATIONAL DEFENSE RESEARCH COMMITTEE
DIVISION SIX - SECTION 6.1

PRESSURE DISTRIBUTION MEASUREMENTS
ON THE
MK 14-1 AND MK 15-1 TORPEDOES

REGRADED UNCLASSIFIED BY ORDER
SEC. ARMY BY Tag per J1918.11

LIBRARY COPY
OF THE
HYDRODYNAMICS LABORATORY
CALIFORNIA INSTITUTE OF TECHNOLOGY
PASADENA 4, CALIFORNIA

LIBRARY COPY
PLEASE RETURN

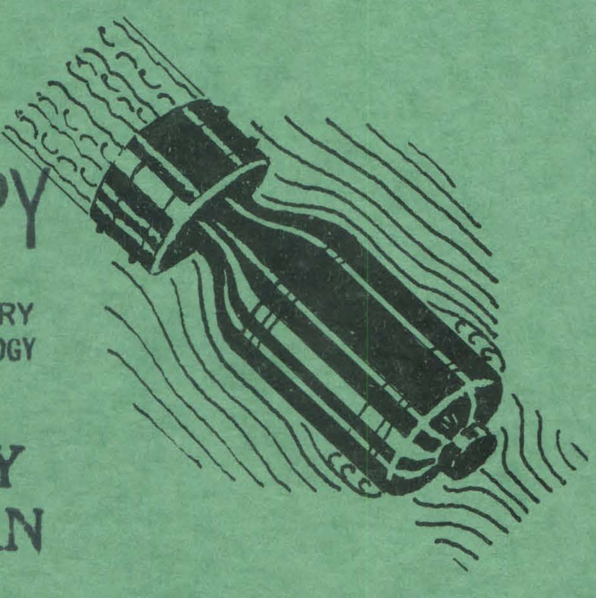

THE HIGH SPEED WATER TUNNEL
CALIFORNIA INSTITUTE OF TECHNOLOGY
PASADENA, CALIFORNIA

LIBRARY COPY
PLEASE RETURN
CONFIDENTIAL

SECTION № 6.1 sr 207-2244
LABORATORY № ND-18.1

COPY № 93

[redacted]

CONFIDENTIAL

OFFICE OF SCIENTIFIC RESEARCH AND DEVELOPMENT
NATIONAL DEFENSE RESEARCH COMMITTEE
DIVISION SIX - SECTION 6.1

PRESSURE DISTRIBUTION MEASUREMENTS ON THE MK 14-1 AND MK 15-1 TORPEDOES

ROBERT T. KNAPP

OFFICIAL INVESTIGATOR

THE HIGH SPEED WATER TUNNEL
AT THE
CALIFORNIA INSTITUTE OF TECHNOLOGY
HYDRODYNAMICS LABORATORY
PASADENA, CALIFORNIA

Section No. 6.1-sr207-2244

Laboratory No. ND-18.1

Report Prepared by
Joseph Levy
Hydraulic Engineer

August 15, 1945

This document contains information affecting the national defense of the United States within the meaning of the Espionage Act, 50 U.S.C., 31 and 32, as amended. The transmission or the revelation of its contents in any manner to an unauthorized person is prohibited by law.

CONFIDENTIAL

TABLE OF CONTENTS

ABSTRACT AND SUMMARY

This report covers measurements of the pressure distribution around the bodies of the Mk-14-1 and Mk 15-1 Torpedoes, both when equipped with the standard tail assembly and with a shroud ring tail added, and includes studies of the effect on the pressure distribution of variations in yaw and pitch angles, velocity, and static pressure (i.e., submergence). These two torpedoes are both 21 inches in diameter, made up with heads and afterbodies having the same external shape, and both are equipped with identical fin and rudder assemblies. The only difference between their external shapes, therefore, is due to the different lengths of cylindrical mid-sections, and resultant different over-all lengths. (The Mk 14-1 is 20.5 ft long, and the Mk 15-1 is 24 ft long). The tests were made on 2-inch diameter models (model scale 1:10.5).

In addition to providing a general picture of the pressure distribution as affected by the different variables, the data presented herein are useful in determining the best locations and arrangements for the pressure intakes to the immersion mechanism and to the depth and roll recorder, and also as a check on cavitation measurements. Because the pressures on the fins themselves were not measured in these tests, the data cannot be used to calculate the over-all forces acting on the complete torpedo.

The main observations and conclusions are summarized in the following paragraphs:

1. Within the range of these tests, the pressure distribution, as presented in terms of p/q, was found to be independent of variations in velocity and static pressure or submergence. That is, the difference between the pressure at any station on the body and the static pressure of the undisturbed water is independent of the static pressure and is directly proportional to the velocity head.

2. The addition of the shroud ring around the fins of these torpedoes has no measurable effect on the pressure distribution.

3. The pressure distributions around the head and afterbody of the Mk 15-1 were found to be practically identical with those of the Mk 14-1. That is, increasing the length of the cylindrical mid-section does not, in this case, affect the pressure distribution on the head or afterbody.

4. The pressure on the surface of these torpedoes equals the static pressure of the undisturbed water at two positions, one on the projectile nose and one on the afterbody. (See Figures 12, 18, 24, and 30). Ahead and behind these

two stations the pressure is above static, while between the two (which includes about 83% of the over-all length of the Mk 14-1, and 86% on the Mk 15-1) the pressure is below static.

5. The position on the afterbody at which $P = P_o$ is only slightly affected by yaw or pitch angles up to 3^o.

6. On the basis of these measurements, made without rotating propellers, it appears that the best arrangement for the pressure intake to the immersion mechanism would be through a piezometer ring connecting to four pressure taps uniformly distributed about the circumference of the afterbody and about 35 inches ahead of the end of the tail. The pressure imposed on the diaphragm would then be equal to true hydrostatic pressure, and practically independent of yaw or pitch. The influence of the propellers may shift this point slightly either aft or forward.

7. Placing the pressure take-off for the depth and roll recorder where $P = P_o$ on the nose is not recommended because P changes rapidly in this zone and large errors can result from small inaccuracies in locating the connection. Connection of the depth and roll recorder to the point of the afterbody where $P = P_o$ is, of course, physically impracticable. It is recommended, therefore, that the pressure intake be left unchanged and, if necessary, determine the corrections to be applied to the depth record.

PRESSURE DISTRIBUTION MEASUREMENTS
ON THE
MK 14-1 AND MK 15-1 TORPEDOES

INTRODUCTION

This report is the second in a series covering Water Tunnel tests on the United States Navy Torpedoes Mk 14, Modification 1, and Mk 15, Modification 1. The first report(1) included force and cavitation measurements on the standard torpedoes and on these torpedoes when equipped with a proposed shroud ring tail. The tests reported herein were made to investigate the pressure distribution about the bodies of these torpedoes, both with the standard tail and with a shroud ring tail, and to study the effect on the pressure distribution of variations in velocity, static pressure (submergence), and orientation with respect to the line of travel. The tests were made on 2-inch diameter models in the High Speed Water Tunnel at the California Institute of Technololgy, and were authorized by Dr. E. H. Colpitts, Chief of Section 6.1, National Defense Research Committee, in a letter dated July 12, 1944.

The data presented herein are useful for determining the best location for the pressure intake to the depth control (immersion) diaphragm, and for determining whether the location of the depth and roll recorder is such as to enable the device to indicate actual running depth. The data may also be used to check the cavitation characteristics of the torpedoes.

The tests made included measurements of the pressure distribution about the Mk 14-1 and Mk 15-1 Torpedoes with standard tail, and also with tail fitted with the proposed ring tail, under conditions of constant velocity and constant static pressure, and with varying yaw between -6 and +6 degrees. Additional tests were made to determine the effect, if any, of variations in static pressure and velocity on the pressure distribution.

APPARATUS AND TEST PROCEDURES

DESCRIPTION OF THE TORPEDOES

The Mk 14 and Mk 15 series torpedoes are all 21 inches in diameter, made up with heads and afterbodies having the same external shape, and all are equipped with identical fin and rudder assemblies. The only differences in their external shapes, therefore, are due to the different lengths of cylindrical mid-sections,

(1) "Force and Cavitation Tests of the Mk 14-1 and Mk 15-1 Torpedoes" by Joseph Levy, NDRC Section No. 6.1-sr207-2238, July 15, 1945

and resultant different over-all lengths, of the various modifications of these two groups. To reduce the bulk of the work it was decided to make these tests on only one torpedo in each of the two groups. The Mk 14, Modification 1, and Mk 15, Modification 1, were selected because it was understood that these were the most frequently used. The general outline, overall dimensions, and weights and displacements of these two prototype torpedoes are shown in Figure 1. Figure 2 shows the fin and rudder structures,

	MK 14-1	MK 15-1
WEIGHT READY FOR WAR SHOT	3185 ± 20 LBS.	3847 ± 20 LBS.
WEIGHT READY FOR EXERCISE SHOT	3071 ± 20 LBS.	3847 ± 20 LBS.
DISPLACEMENT (AT 64 LBS/CU. FT.)	2516 LBS.	3045 LBS.
WETTED SURFACE	103.3 SQ. FT.	122.5 SQ. FT.

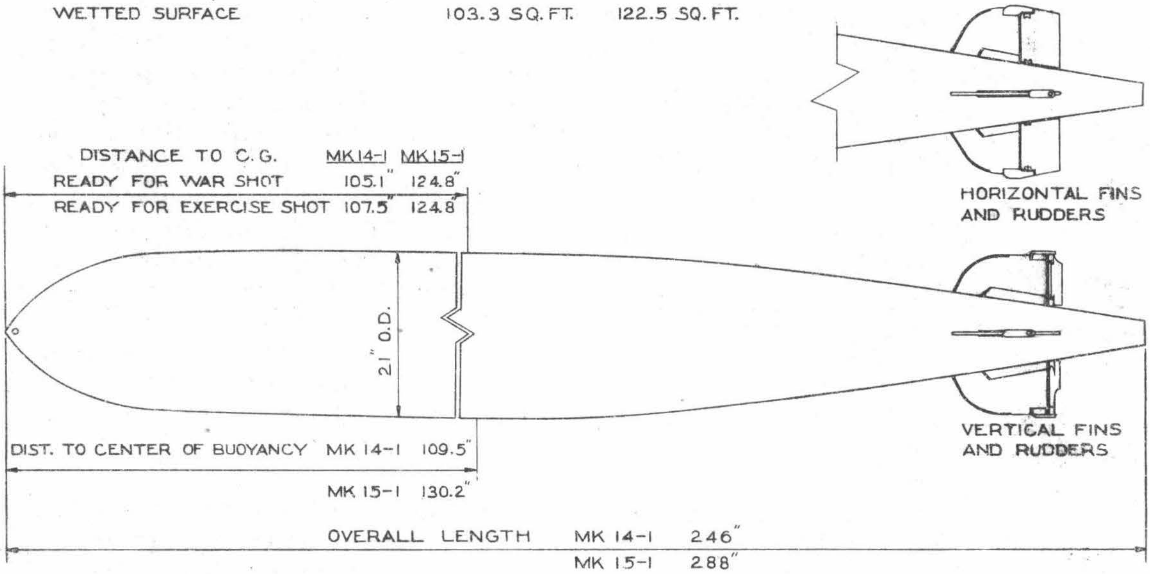

FIG. 1 - MK 14-1 AND MK 15-1 TORPEDOES
PRINCIPAL DIMENSIONS AND WEIGHTS

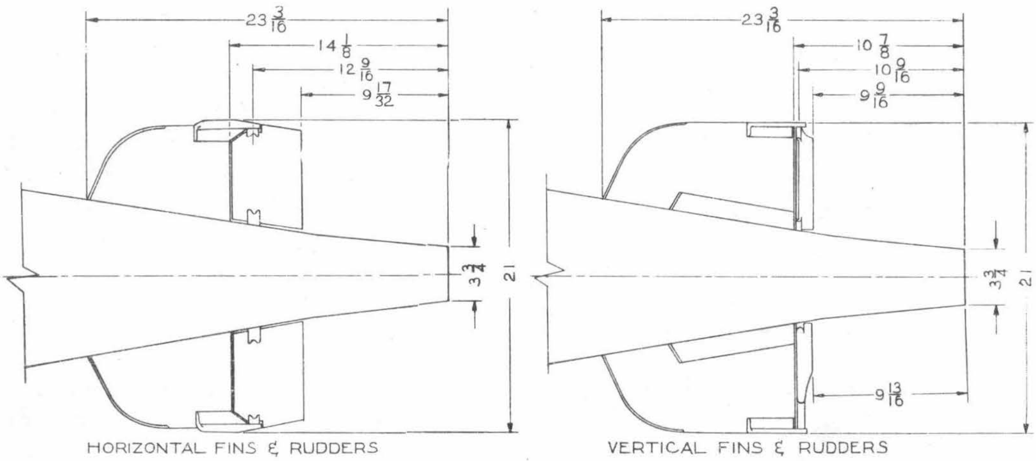

FIG. 2 - TAIL SURFACES OF MK 14-1 AND MK 15-1 TORPEDOES

Figure 3 shows the shroud ring installed, and the profile of the proposed shroud ring is shown in Figure 4. The location of the pressure taps is shown in Figure 5.

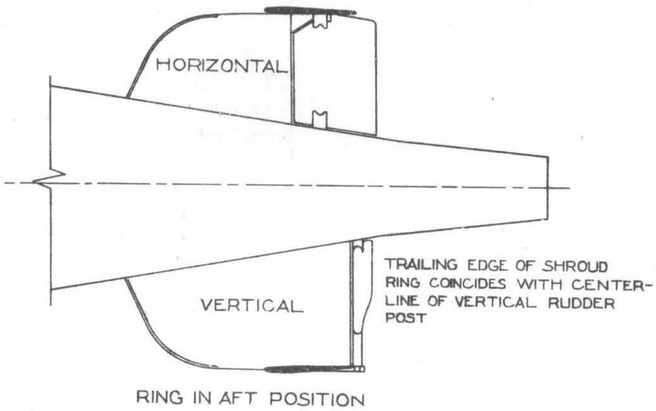

FIG. 3 - TAIL OF MK 14-1 AND MK 15-1 TORPEDOES SHOWING LOCATION OF SHROUD RING

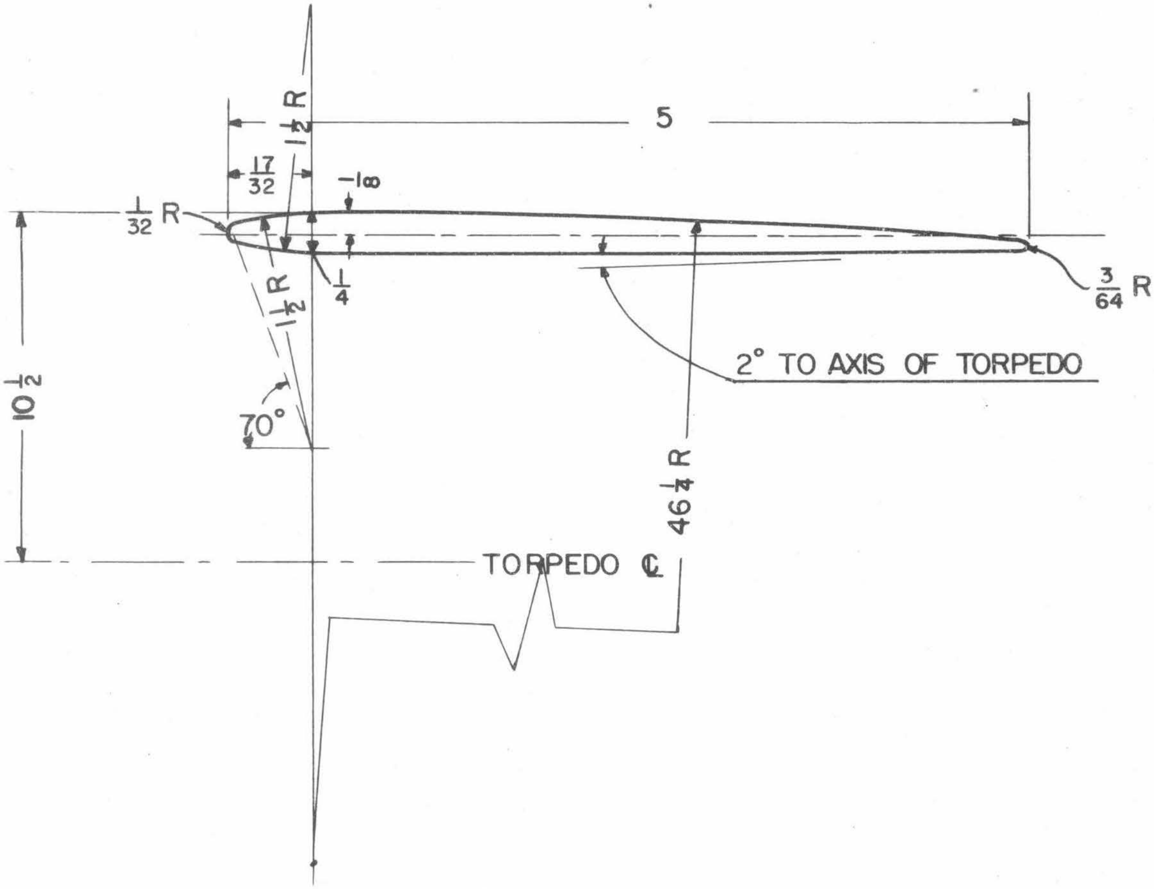

FIG. 4 - PROFILE OF PROPOSED SHROUD RING

CONFIDENTIAL

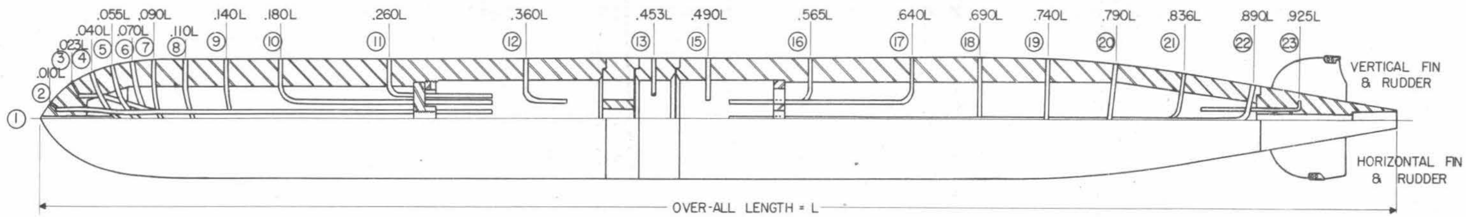

MK 14-1 TORPEDO MODEL

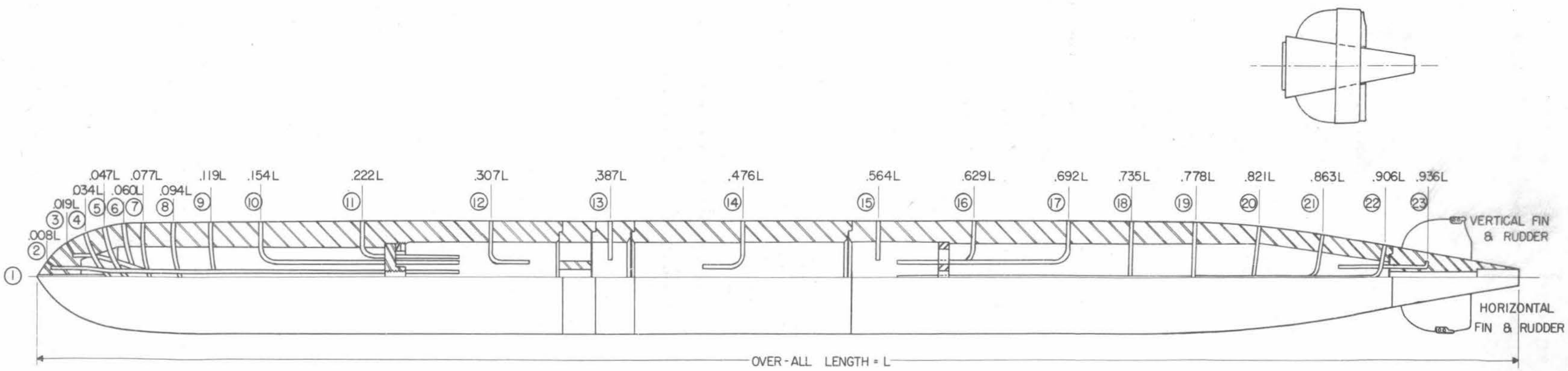

MK 15-1 TORPEDO MODEL

FIG. 5 — SHOWING LOCATION OF PRESSURE TAPS

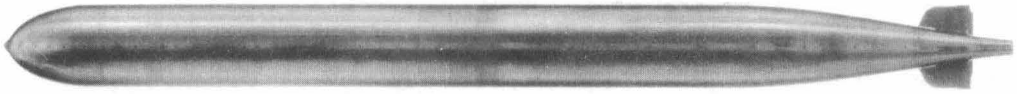

FIG. 6 — MODEL OF MK 14-1 TORPEDO WITH STANDARD TAIL

FIG. 7 — MODEL OF MK 14-1 TORPEDO WITH RING TAIL

FIG. 8 — MODEL OF MK 15-1 TORPEDO WITH STANDARD TAIL

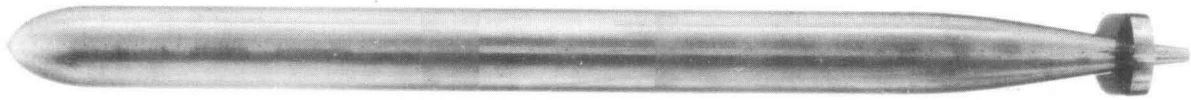

FIG. 9 — MODEL OF MK 15-1 TORPEDO WITH RING TAIL

MODEL CONSTRUCTION

The stainless steel models used in these tests are shown in Figures 6 to 9, inclusive, and have a maximum diameter of two inches (model scale ratio 1 to 10.5). Since both prototypes have identical heads and afterbodies, it was necessary to make only one model head and one model afterbody. A removable length of cylindrical mid-section provides for the change in over-all length in going from one model to the other. Two interchangeable tail cones were provided, one with fins and rudders but without shroud ring, and one with shroud ring. The rudders on both tail cones are fixed in neutral position. The forebody, afterbody, and tail cones were so made that each part could be rotated about the longitudinal axis independently of the other parts. With this arrangement, a single row of piezometer openings distributed along a meridian is sufficient for exploring the pressure distribution about the entire body. A protractor scale scribed at the joint line of each body section, graduated in 5-degree intervals, provides the means for setting the angular position of the piezometer taps.

PIEZOMETER OPENINGS AND PRESSURE LEADS

The piezometer openings were made by drilling 1/16-inch holes at right angles to the surface before making the final finishing cut on the outside. Each hole was then plugged with a stainless steel rod extending about 3/16 inch into the body. A brass tube of 1/16-inch outside diameter and 1/32-inch inside diameter was inserted in the hole from the inside and silver-soldered in place. A finishing cut was then taken over the entire surface and a 1/32-inch diameter hole was drilled through each plug and its lip was reamed to a 0.005-inch radius. Twenty-two such openings were provided on the Mk 14-1 model, and 23 on the Mk 15-1 model. As will be seen in Figure 5, Tap 14 is located in the mid-section piece which is used with the Mk 15-1 model alone.

Rubber tubes were used to connect these brass tubes to a bundle of nickel-silver tubes extending from the outside of the Water Tunnel, through the model supporting strut, and into the model through an opening in the bottom of the center section. The slenderness of the strut limited the number of tubes that could be carried through it to 12. It was necessary, therefore, to measure the pressure distribution about the forebody and about the afterbody in separate test runs. Outside the working section, each tube terminated in a valve mounted on a common manifold, so that each piezometer tap could, in turn, be connected to the differential pressure gage. Figure 10 shows the model of the Mk 14-1 mounted on the streamlined strut, with base plate and tube manifold, ready for installation in the tunnel.

DIFFERENTIAL PRESSURE GAGE

The differential pressure gage used in these tests consists of two opposed piston and cylinder units and an automatically weighing beam type balance. The two opposing pistons are interconnected with a yoke system which also connects to the beam of the balance. Thus, the force transmitted to the balance is proportional to the difference between the pressures applied against the two pistons. The cylinders are continuously rotated by an electirc motor to overcome static friction. Another motor, controlled through a photo-electric cell by the rise and fall of the balance beam, shifts a rider weight along the beam to balance the applied force. A veeder counter connected to the rider drive is geared to read the differential pressure directly in pounds per square inch to 0.001 psi.

TEST PROCEDURE

The pressure distribution around the torpedo was explored by setting the piezometer openings at a given angle and measuring the pressures at each tap for yaw angles of 0, $\pm$ 3, and $\pm$ 6 degrees. For the Mk 14-1, the piezometer tap settings were varied from 0 to 90 degrees in 15-degree steps. Because of the symmetry of the torpedo, these measurements give the pressure distribution about the entire body. For the Mk 15-1, measurements were made for pressure tap settings of 0, 45, and 90 degrees only. Most of the

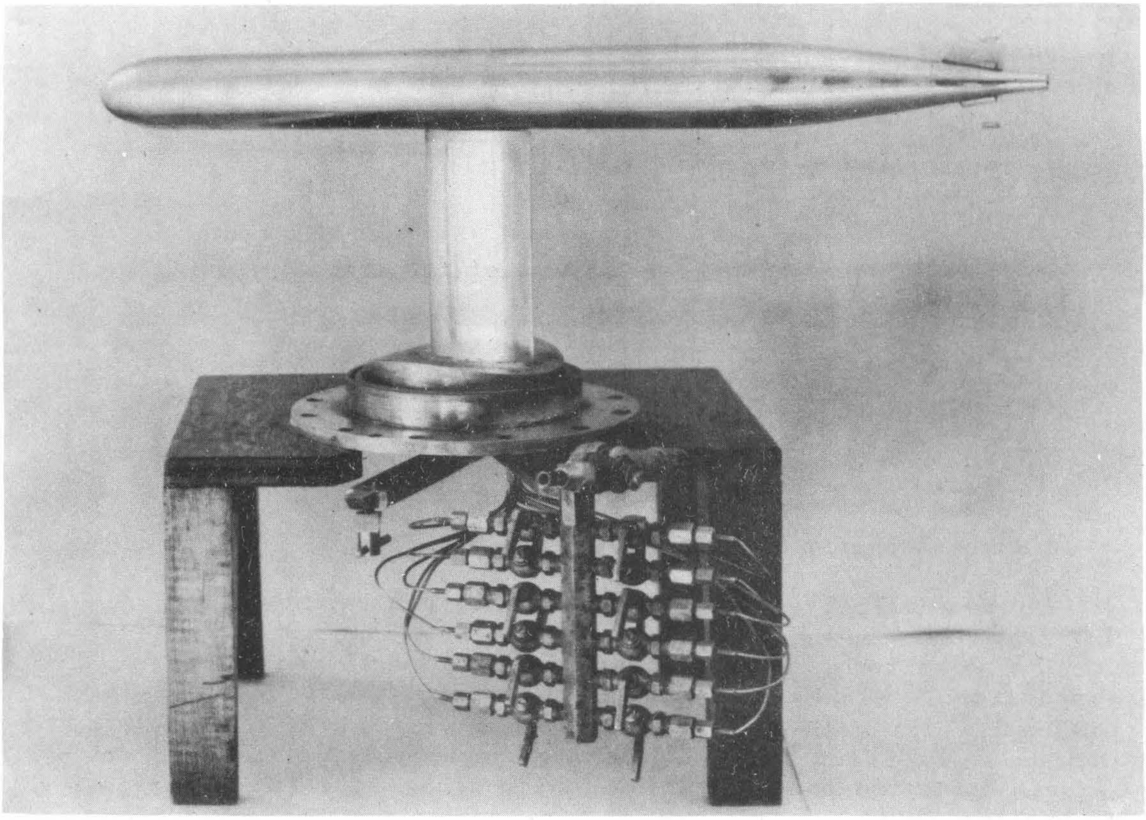

FIG. 10 – MODEL OF MK 14-1 TORPEDO ASSEMBLED ON STREAMLINED STRUT WITH BASE PLATE AND TUBE MANIFOLD READY FOR INSTALLATION IN THE TUNNEL

tests were made with a constant velocity of 40 feet per second and constant static pressure in the tunnel working section of 10 psi. Several test runs were made with different velocities and static pressures to determine the effect of these variables on the pressure distribution.

The static pressure reference was taken at the tunnel wall at a point 3 model diameters upstream of the model nose. The differential pressure measured at each piezometer opening was corrected for tunnel pressure gradient by subtracting from it the tunnel pressure drop, measured in the absence of the model, between the reference point and a point opposite that piezometer opening.

TEST RESULTS

PRESENTATION

The test results are shown in Figures 12 to 39, inclusive, and are presented in terms of p/q, where

$p = P - P_o$

P = normal pressure on the surface of the torpedo, pounds per square foot

P_o = static pressure in undisturbed water at same level as torpedo center line, pounds per square foot

$q = 1/2\ \rho\ V^2$ = dynamic pressure of water, pounds per square foot

ρ = mass density of water, slugs per cubic foot

V = mean relative water velocity, feet per second

The tests reported herein include, in effect, measurements on four bodies: (1) Mk 14-1 with standard tail, (2) Mk 14-1 with ring tail, (3) Mk 15-1 with standard tail, and (4) Mk 15-1 with ring tail. The test results, however, show practically identical pressure distributions around the four bodies. That is, increasing the length of the cylindrical mid-section does not affect the pressure distribution on the head or afterbody. Also, the addition of the shroud ring does not alter the pressure distribution. Figure 11 is a composite curve showing the longitudinal pressure distributions at zero yaw on the heads and afterbodies of the four torpedo shapes tested. At the top of the sheet is a half outline of the head and afterbody used with all Mk 14 and Mk 15 series torpedoes, drawn to scale. Distances are measured from the nose and from the tail toward the center in inches, prototype dimensions. The points plotted on the curve are average points for each pressure tap taken from Figures 12, 18, 24, and 30. It is seen that the pressure at each tap is practically the same for both the Mk 14-1 and Mk 15-1, whether without or with the ring tail.

The longitudinal pressure distribution curves presented hereafter are organized in four groups, one for each of the four bodies tested. In the following paragraphs, reference will be made to the figure numbers showing curves for the Mk 14-1 with standrad tail (without ring). The figure numbers given in parentheses refer to the corresponding curves for the three other bodies.

LONGITUDINAL PRESSURE DISTRIBUTION — ZERO YAW

In Figure 12 (18, 24, 30) is shown the longitudinal pressure distribution around the torpedo at zero yaw, plotted against distance from the tip of the nose divided by the over-all length. It is evident that, for a symmetrical body oriented with its axis

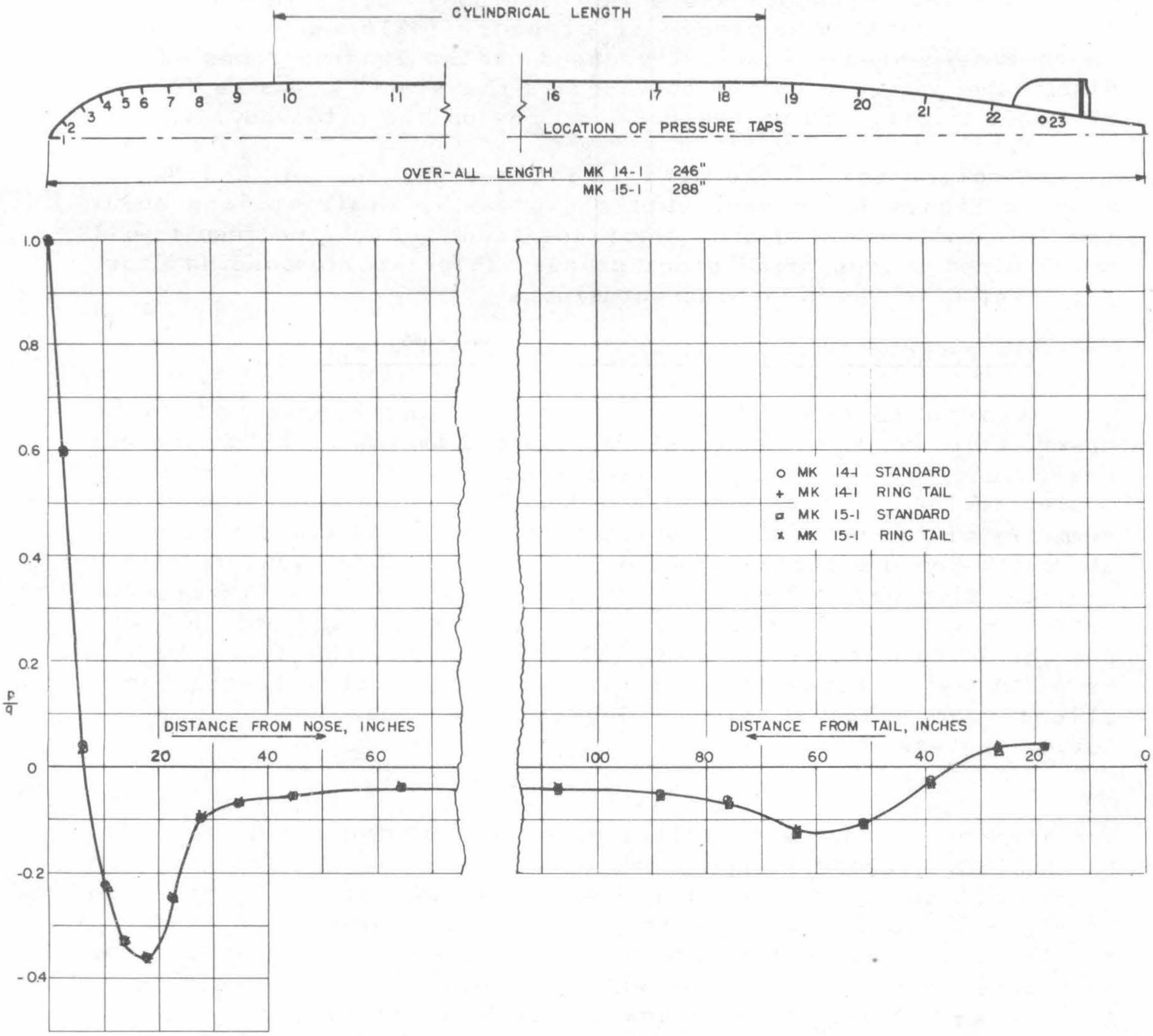

FIG. 11 - MK 14-1 AND MK 15-1 TORPEDOES
LONGITUDINAL PRESSURE DISTRIBUTION
ON HEAD AND AFTERBODY
YAW ANGLE = 0^{o}

parallel to the direction of motion, the pressure around any section normal to the axis should be constant. It is seen that the seven points plotted for each pressure tap on the Mk 14-1, and the three points per tap on the Mk 15-1, indeed show very little scatter, except for Tap No. 15 on the Mk 14-1. This tap is immediately behind the joint between the center-section and the afterbody, as may be seen in Figure 5. Apparently the after edge of the center section had been roughened slightly from continued use, and this roughness affected the pressure readings at Tap 15.

From full stagnation pressure at the tip of the nose, the pressure drops rapidly to about 0.36 q below static and then rises again, but remains below static pressure over almost the entire length of the torpedo. Where the afterbody begins to taper down there is a further decrease in pressure followed by a rise to above static pressure slightly ahead of the leading edges of the fins. The pressure on the body equals the static pressure ($P = P_o$) at two stations, one on the nose and one on the afterbody.

A comparison of the data of Figures 12, 18, 24, and 30 was made in Figure 11 to show that the pressure distributions about the four bodies tested are nearly identical. The same result will be obtained by comparing other groups of four corresponding drawings listed in the following paragraphs.

YAW EFFECTS ON LONGITUDINAL PRESSURE DISTRIBUTION

Figure 13 (19, 25, 31) shows the longitudinal pressure distribution on the body as it is affected by yaw or pitch. These curves show the pressure along a longitudinal section at right angles to the plane of yaw or pitch. From a consideration of the symmetry of the body, it is evident that the pressure distribution along the top and bottom meridians when the torpedo yaws to either starboard or port, is exactly the same as the pressure distribution along the sides (on the horizontal meridians) of the torpedo as it pitches up or down. It is seen that the effect of yaw or pitch is to lower the pressure over the entire length, only slightly for angles below 3 degrees, and more noticeably for larger angles.

In Figures 14 (20, 26, 32) and 15 (21, 27, 33) is shown the longitudinal pressure distribution on the windward and lee sides of the body, respectively, along meridians at 45 degrees with the planes of yaw or pitch. It is seen that yaw causes the pressure on the nose to increase on the windward side and to decrease on the lee side. Along the mid-portion of the hull, the pressure on both sides decreases slightly with yaw, and on the afterbody taper the pressure decreases with yaw or pitch on the windward side and increases on the lee side. In the vicinity of the tail fins (at Taps 22 and 23), the pressures are affected by the fins, and on the lee side the direction of change in pressure due to yaw is again reversed.

Figures 16 (22, 28, 34) and 17 (23, 29, 35) show the longitudinal pressure distribution along the windward and lee sides of the body, respectively, along a section in the plane of yaw or pitch, i.e., along the top and bottom if pitching, and along the sides when yawing. It is seen that on the nose, the pressure again rises on the windward side and drops on the lee side when the torpedo is yawed. Along the cylindrical portion of the hull, the pressure on the windward side increases with yaw, and on the lee side it is practically unaffected by yaw.

PRESSURES AROUND CROSS SECTIONS NORMAL TO TORPEDO AXIS

In Figures 36 to 39, inclusive, are presented the transverse pressure distributions around cross sections taken normal to the axis of the torpedo at each piezometer opening or station. The curves show the pressures for yaw angles of 0, 3, and 6 degrees, plotted against body angles measured to either side from the vertical center line. Again, from symmetry considerations, it is evident that these curves give also the pressure distribution when the torpedo is pitching, if we measure the angles from the horizontal center line instead of the vertical. Also, the angles may be reckoned from either end of the center line (i.e., either from top or bottom, or from port side or starboard side) since the pressure distribution is symmetrical about the 90-degree points on windward and lee sides. Figures 36 and 37 cover the stations on the forebody. Figure 38 gives the pressure distribution on the afterbody with standard tail, and Figure 39 on the afterbody with ring tail. A comparison of these last two figures again shows that the presence of the shroud ring has practically no effect on the pressure distribution

The data presented in these figures were taken on the Mk 14-1 model. Similar curves for the Mk 15-1 cannot be plotted because the measurements on this model were made only with the piezometers at 0, 45, and 90 degrees from the vertical. However, the data available on the Mk 15-1 show that the pressure distribution about it is practically the same as about the Mk 14-1. These curves, therefore, may be considered as applying to the Mk 15-1 also, that is, the curve given for any station on the Mk 14-1 applies also to the station having the same number on the Mk 15-1.

It will be noted that Stations 1, 13, and 14 are not shown on these curves. Station 1 is at the tip of the nose, Station 13 is on the fixed center section which could not be rotated, and Station 14 is on the length of cylindrical body section which was used with the model of the Mk 15-1 but not with the Mk 14-1.

EFFECT OF VELOCITY AND STATIC PRESSURE

The tests presented thus far were all made with a water velocity of 40 feet per second and a static pressure in the working section of the tunnel of 10 pounds per square inch. Another series of tests were made with velocities of 25, 30, and 50 feet per second and static pressures of 5, 15, and 25 pounds per square inch. These tests showed that, within the range investigated, the velocity and static pressure have no measurable effect on the pressure distribution.

CALCULATION OF FORCES FROM PRESSURE DISTRIBUTION

With the pressure distribution about a projectile completely known, it is possible to calculate from the pressure distribution data the form drag (but not skin friction drag), the cross force and the moment acting at any yaw angle by proper integration of the distributed pressure forces. These tests, however, were all made on bodies with tail surfaces, and the pressures on these surfaces themselves were not measured because of the thinness of the plates. Therefore, the forces acting on the torpedoes cannot be calculated from the data presented herein.

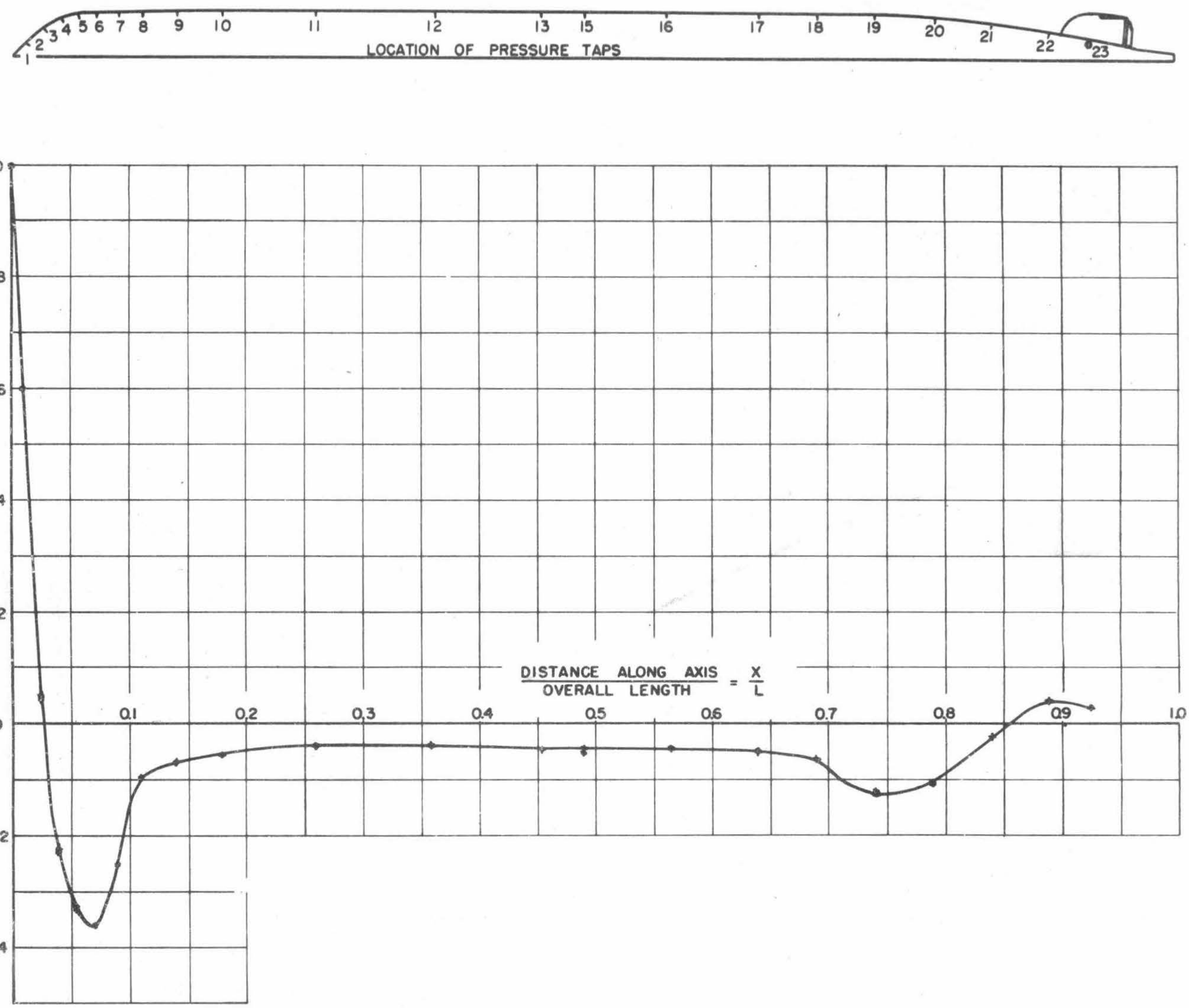

FIG. 12 - MK 14-1 TORPEDO (STANDARD)

PRESSURE DISTRIBUTION
ALONG LONGITUDINAL SECTION

YAW ANGLE = 0^{0}

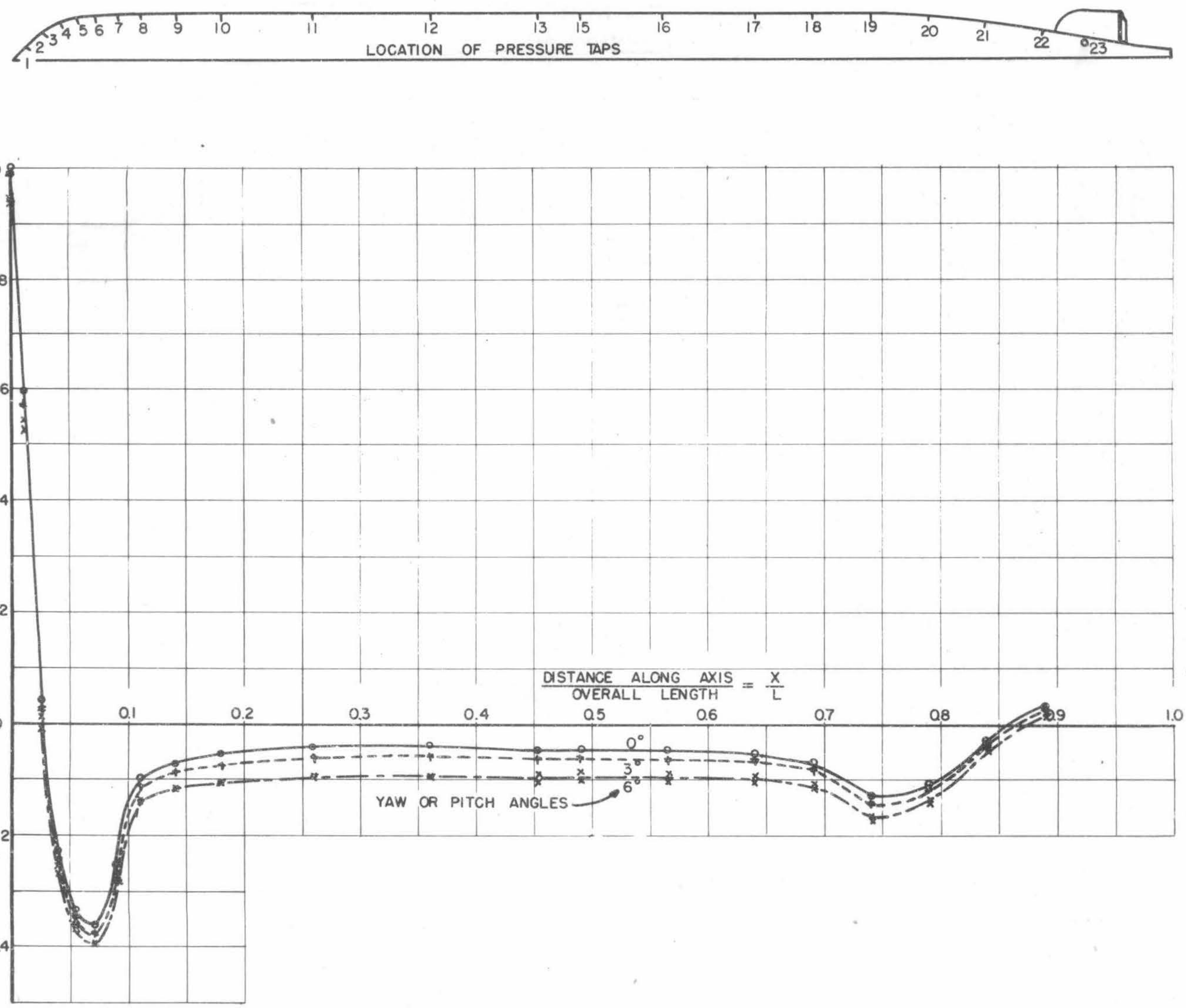

FIG. 13 - MK 14-1 TORPEDO (STANDARD)

PRESSURE DISTRIBUTION
ALONG LONGITUDINAL SECTION
AT RIGHT ANGLES TO PLANE OF YAW OR PITCH

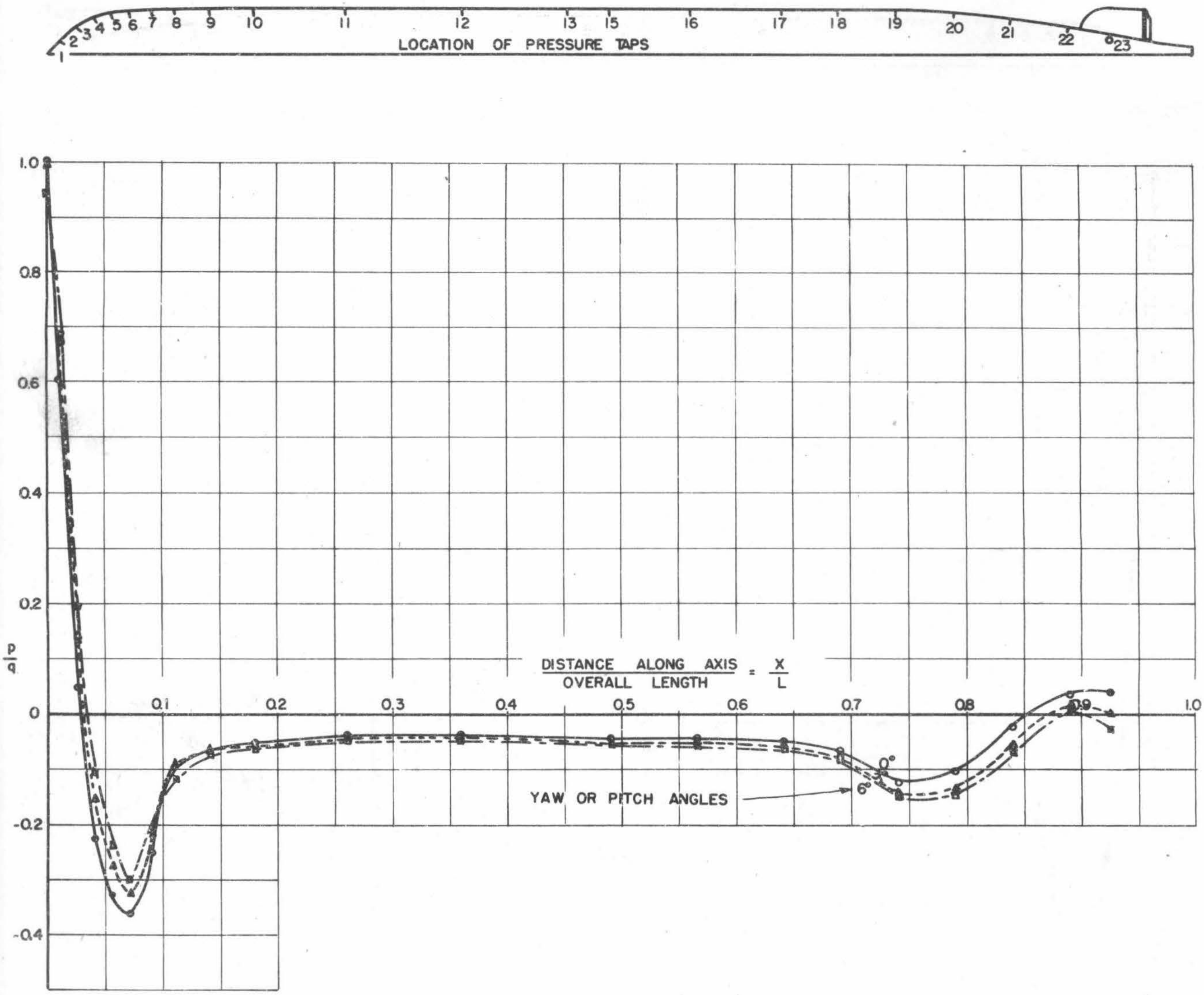

FIG. 14 – MK 14-1 TORPEDO (STANDARD)

PRESSURE DISTRIBUTION
ALONG LONGITUDINAL SECTION
AT 45^{0} TO PLANE OF YAW OR PITCH

Windward Side of Body

CONFIDENTIAL

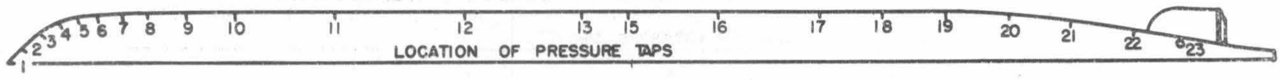

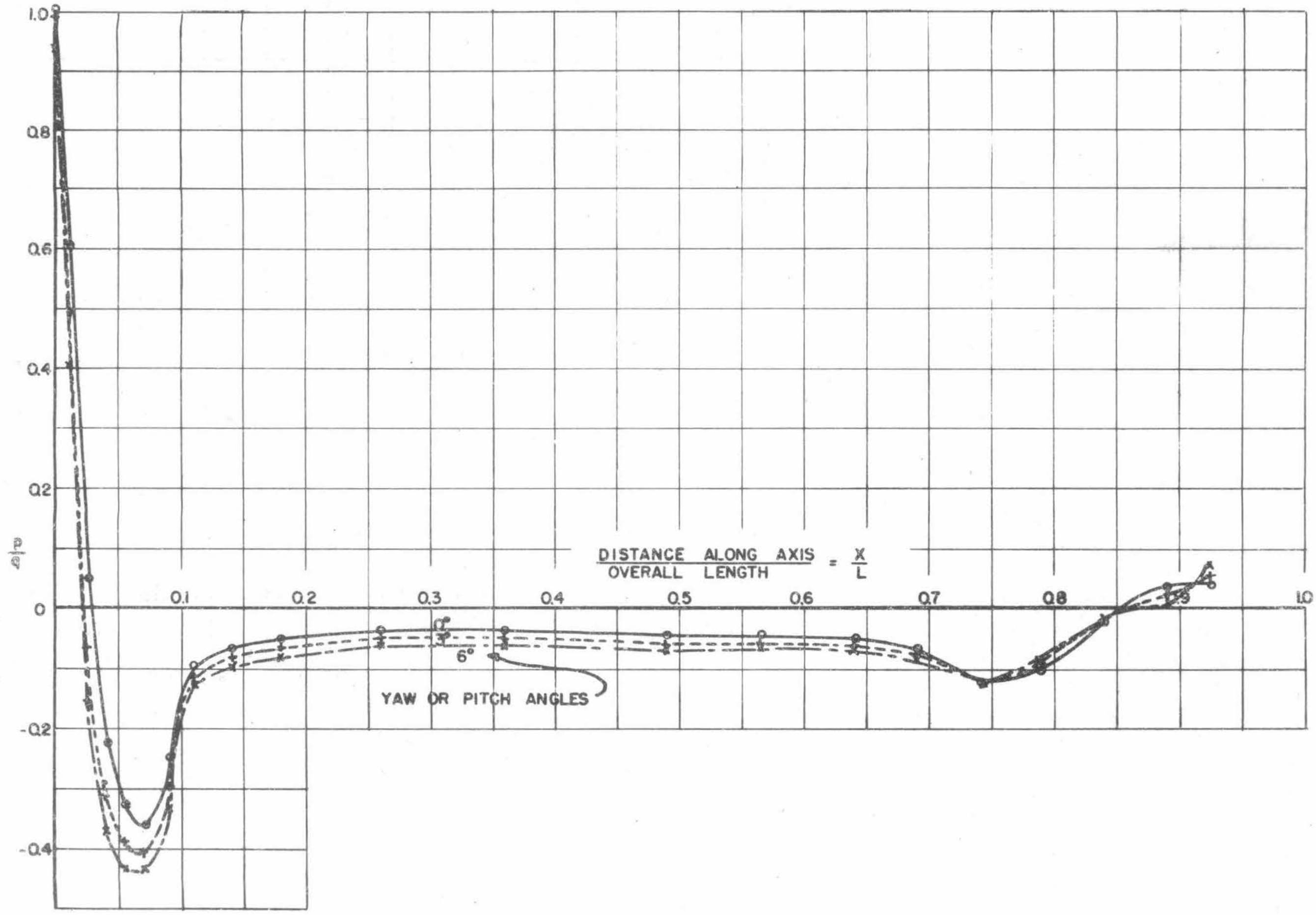

FIG. 15 – MK 14-1 TORPEDO (STANDARD)

PRESSURE DISTRIBUTION
ALONG LONGITUDINAL SECTION
AT 45° TO PLANE OF YAW OR PITCH

Lee Side of Body

CONFIDENTIAL

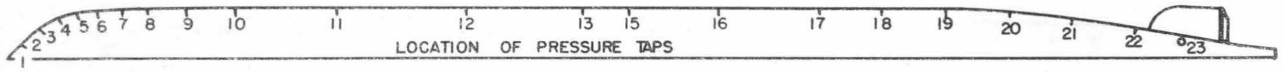

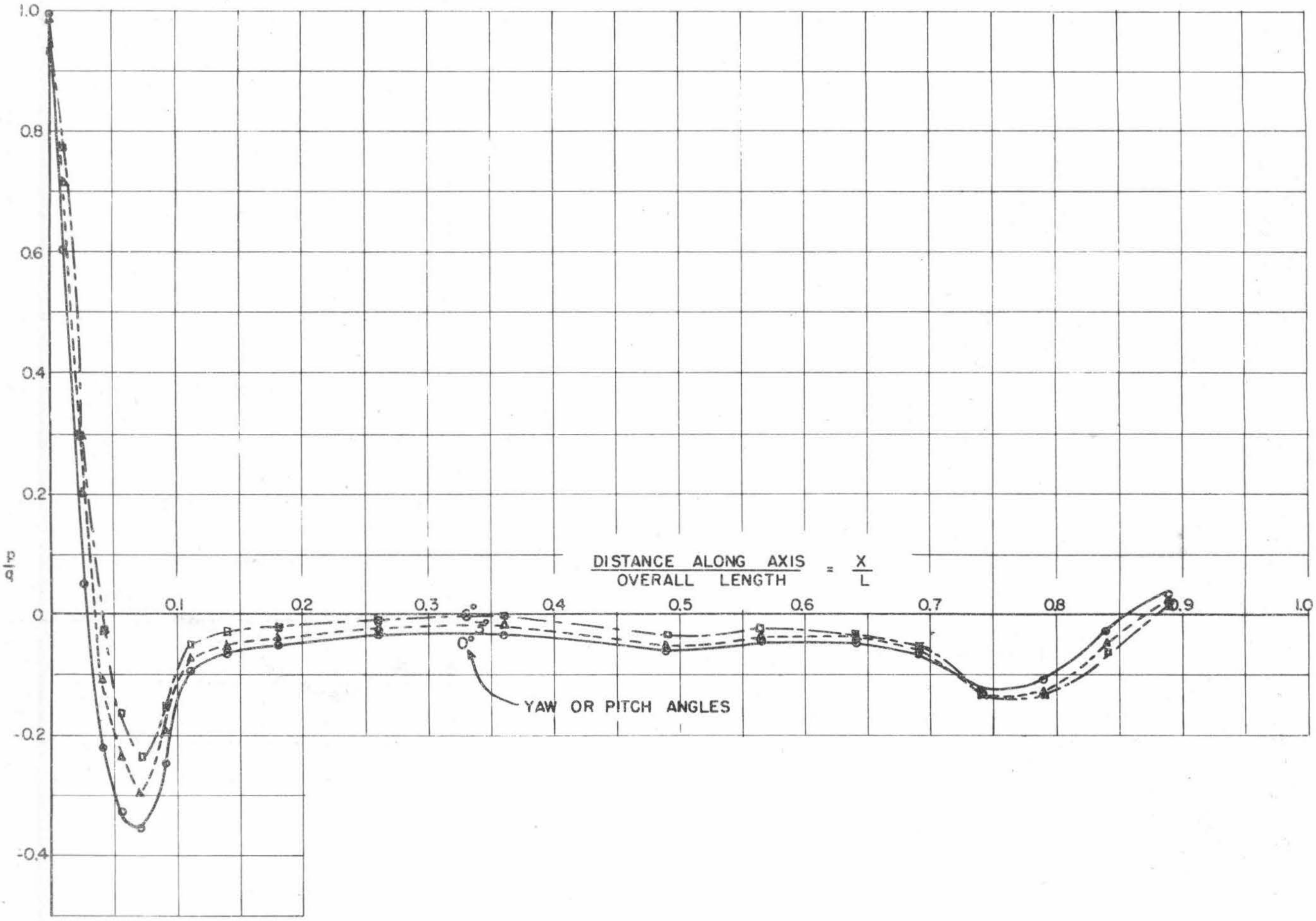

FIG. 16 - MK 14-1 TORPEDO (STANDARD)

PRESSURE DISTRIBUTION
ALONG LONGITUDINAL SECTION
IN PLANE OF YAW OR PITCH

Windward Side of Body

CONFIDENTIAL

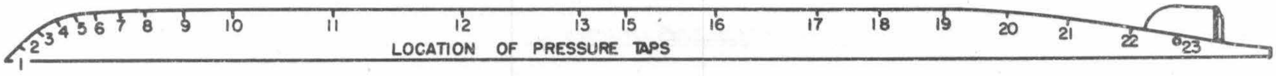

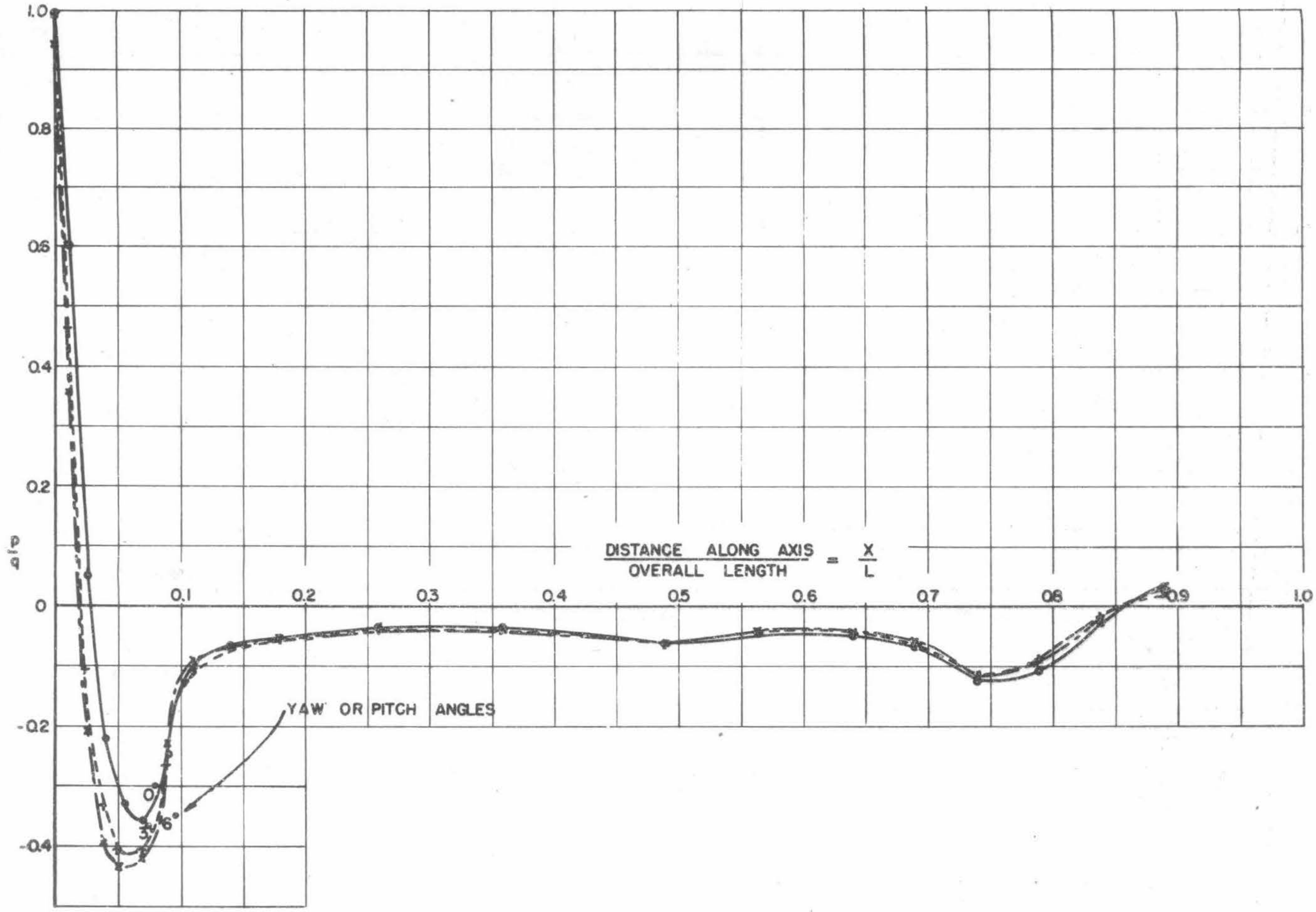

FIG. 17 – MK 14-1 TORPEDO (STANDARD)

PRESSURE DISTRIBUTION
ALONG LONGITUDINAL SECTION
IN PLANE OF YAW OR PITCH

Lee Side of Body

CONFIDENTIAL

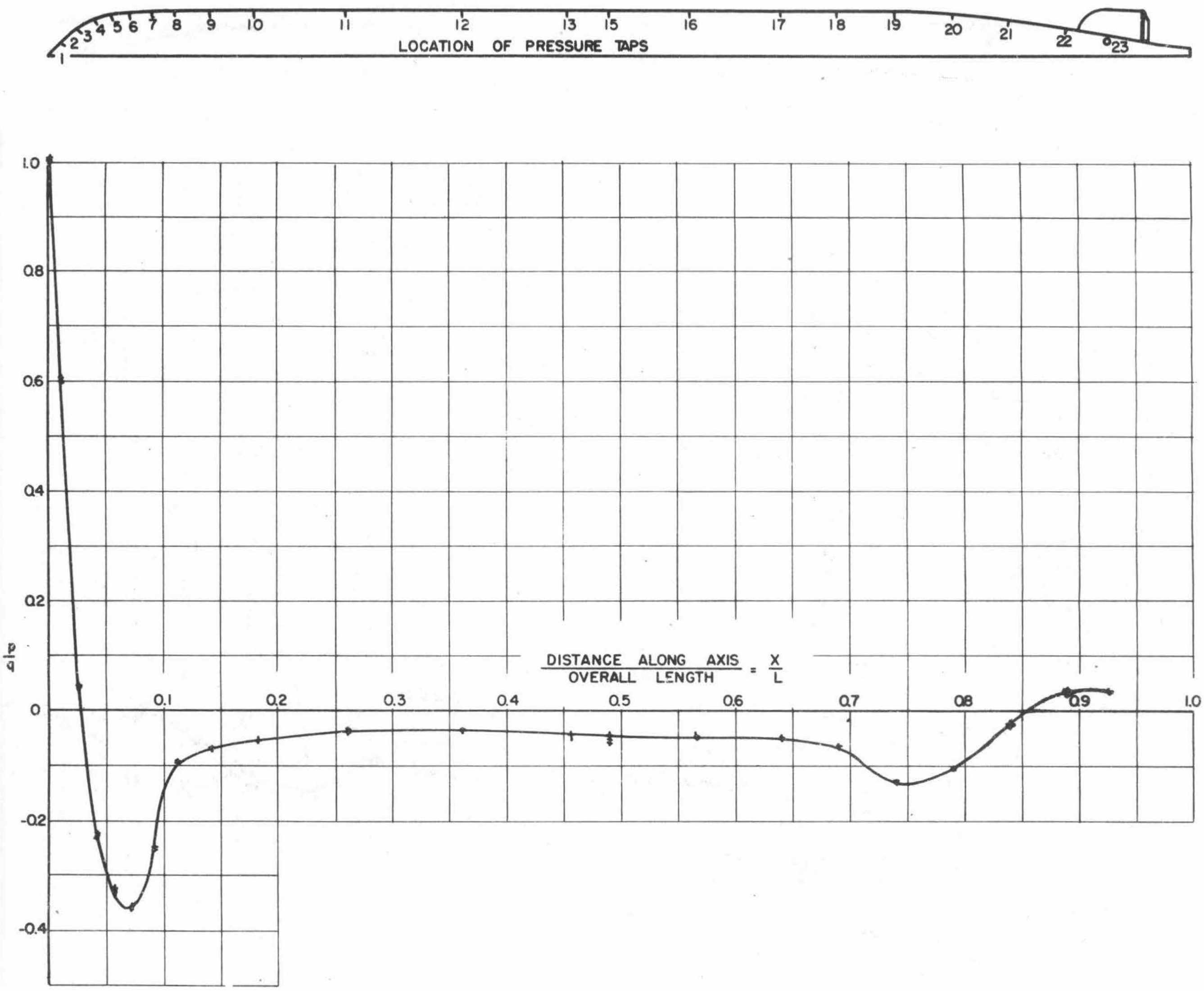

FIG. 18 – MK 14-1 TORPEDO (WITH RING TAIL)

PRESSURE DISTRIBUTION
ALONG LONGITUDINAL SECTION

Yaw Angle = 0^{o}

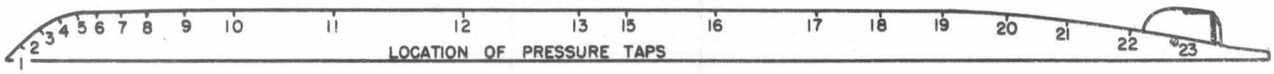

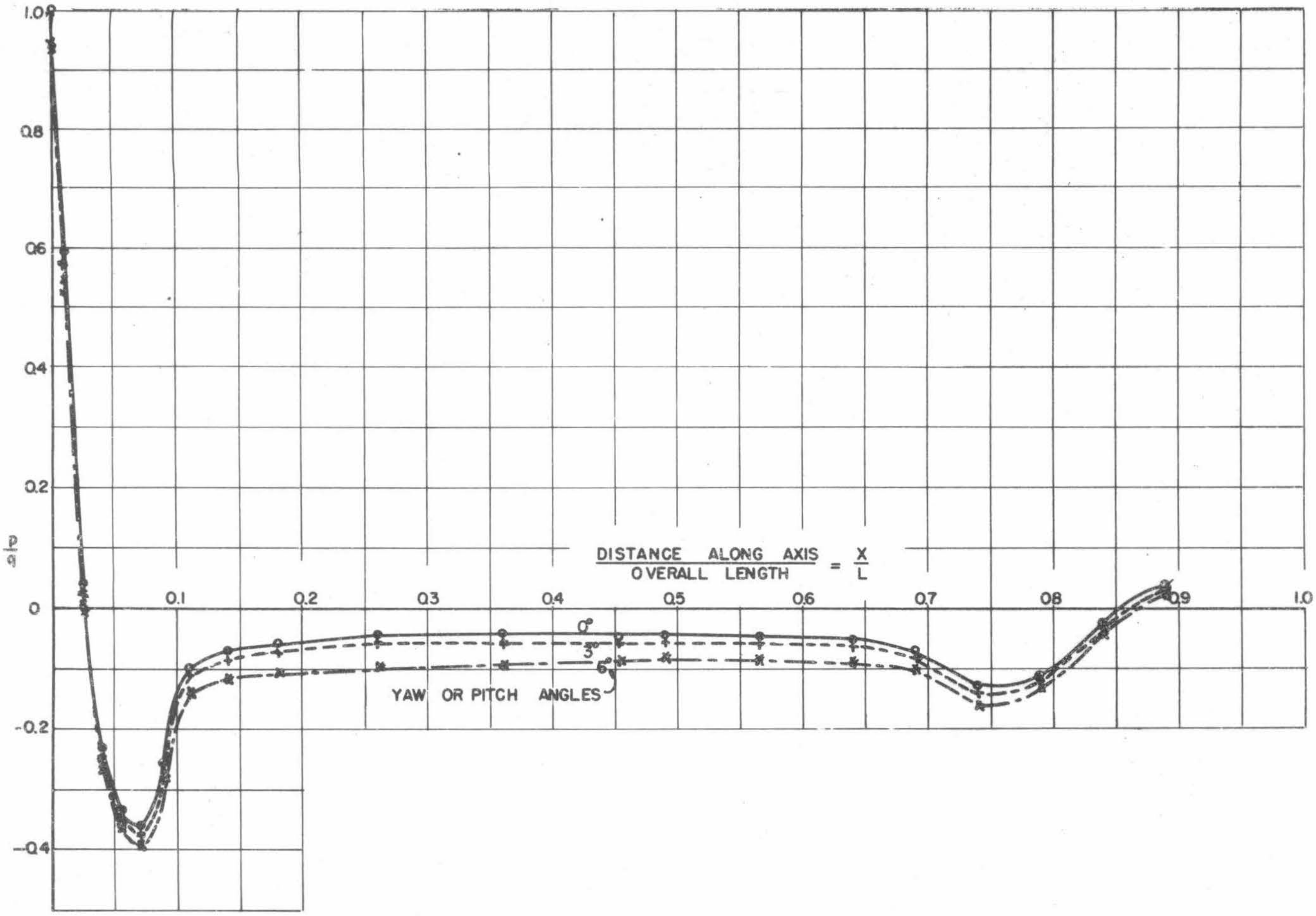

FIG. 19 - MK 14-1 TORPEDO (WITH RING TAIL)

PRESSURE DISTRIBUTION
ALONG LONGITUDINAL SECTION
AT RIGHT ANGLES TO PLANE OF YAW OR PITCH

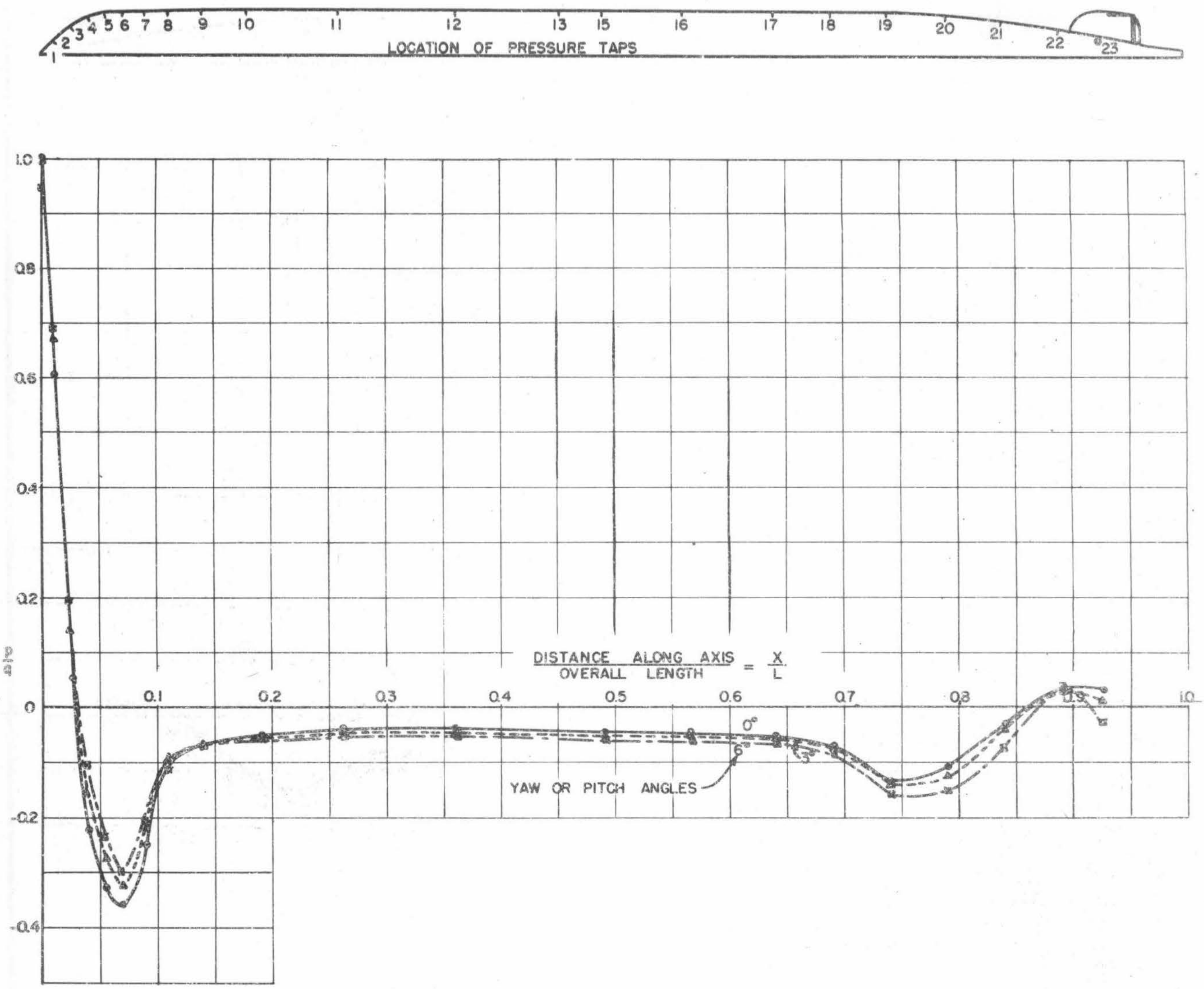

FIG. 20 - MK 14-1 TORPEDO (WITH RING TAIL)

PRESSURE DISTRIBUTION
ALONG LONGITUDINAL SECTION
AT 45^{0} TO PLANE OF YAW OR PITCH

Windward Side of Body

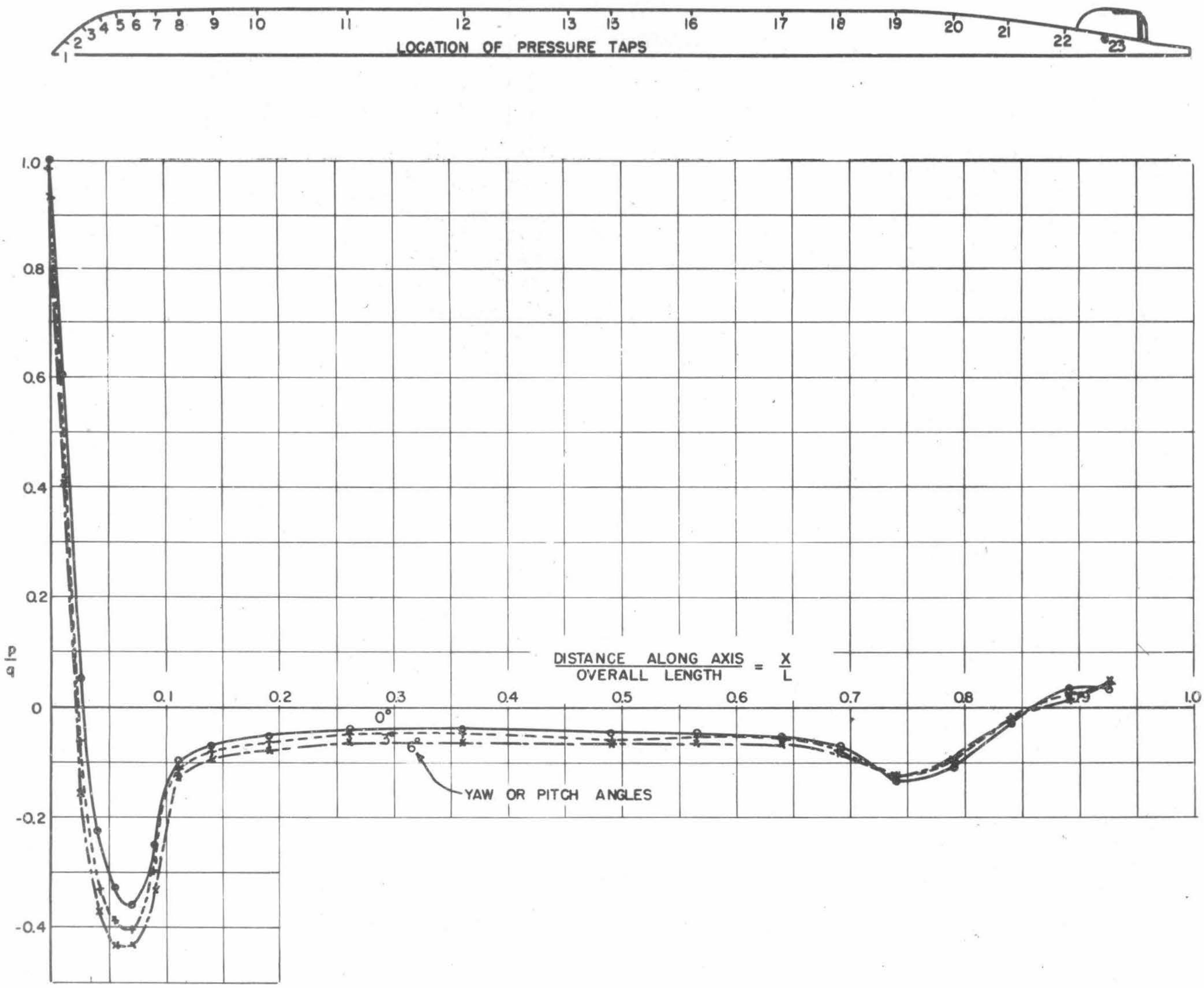

FIG. 21 – MK 14-1 TORPEDO (WITH RING TAIL)

PRESSURE DISTRIBUTION
ALONG LONGITUDINAL SECTION
AT 45° TO PLANE OF YAW OR PITCH

Lee Side of Body

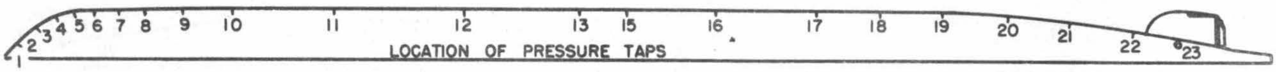

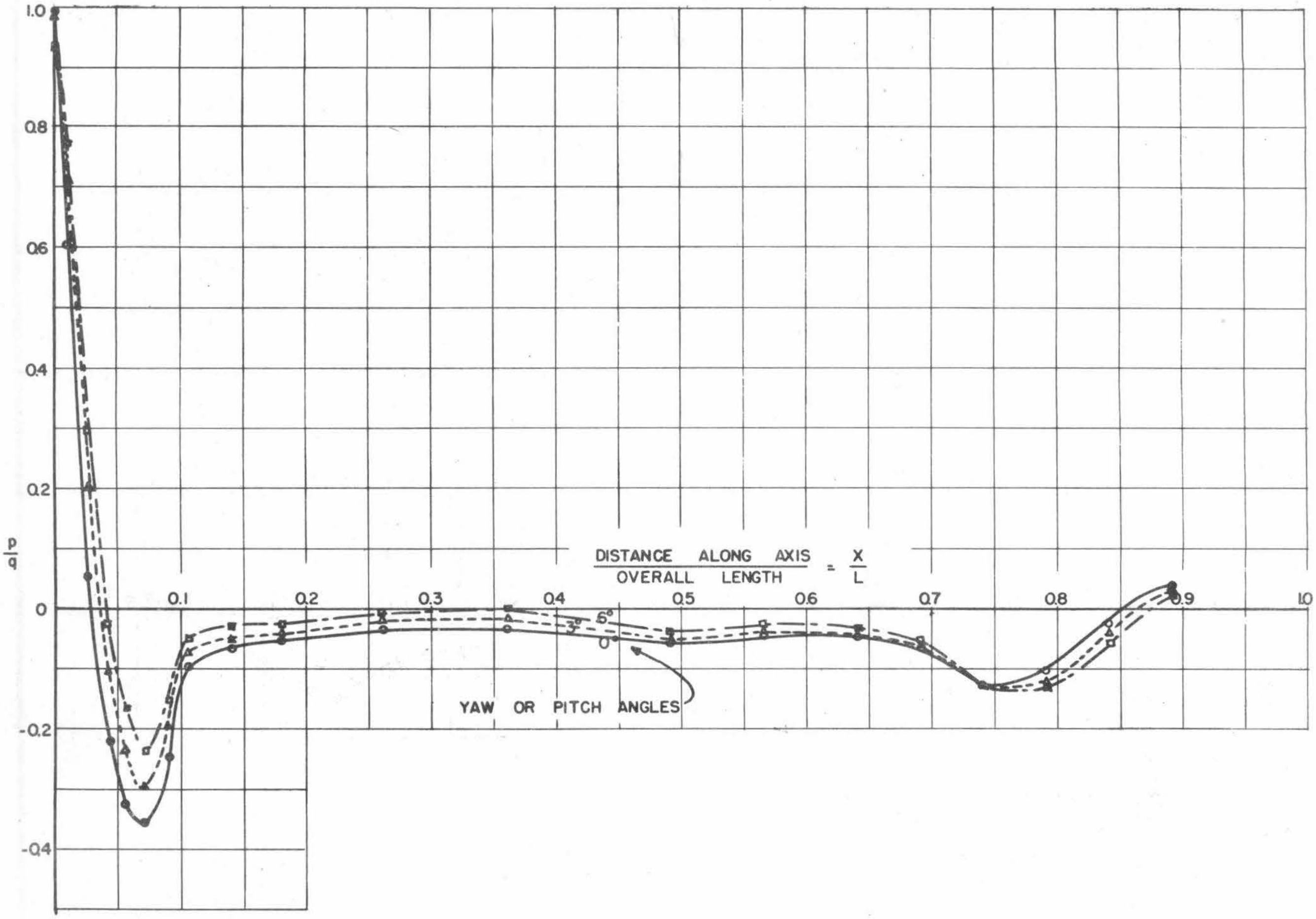

FIG. 22 - MK 14-1 TORPEDO (WITH RING TAIL)

PRESSURE DISTRIBUTION
ALONG LONGITUDINAL SECTION
IN PLANE OF YAW OR PITCH

Windward Side of Body

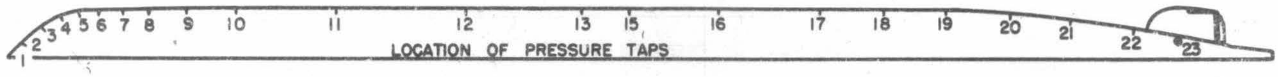

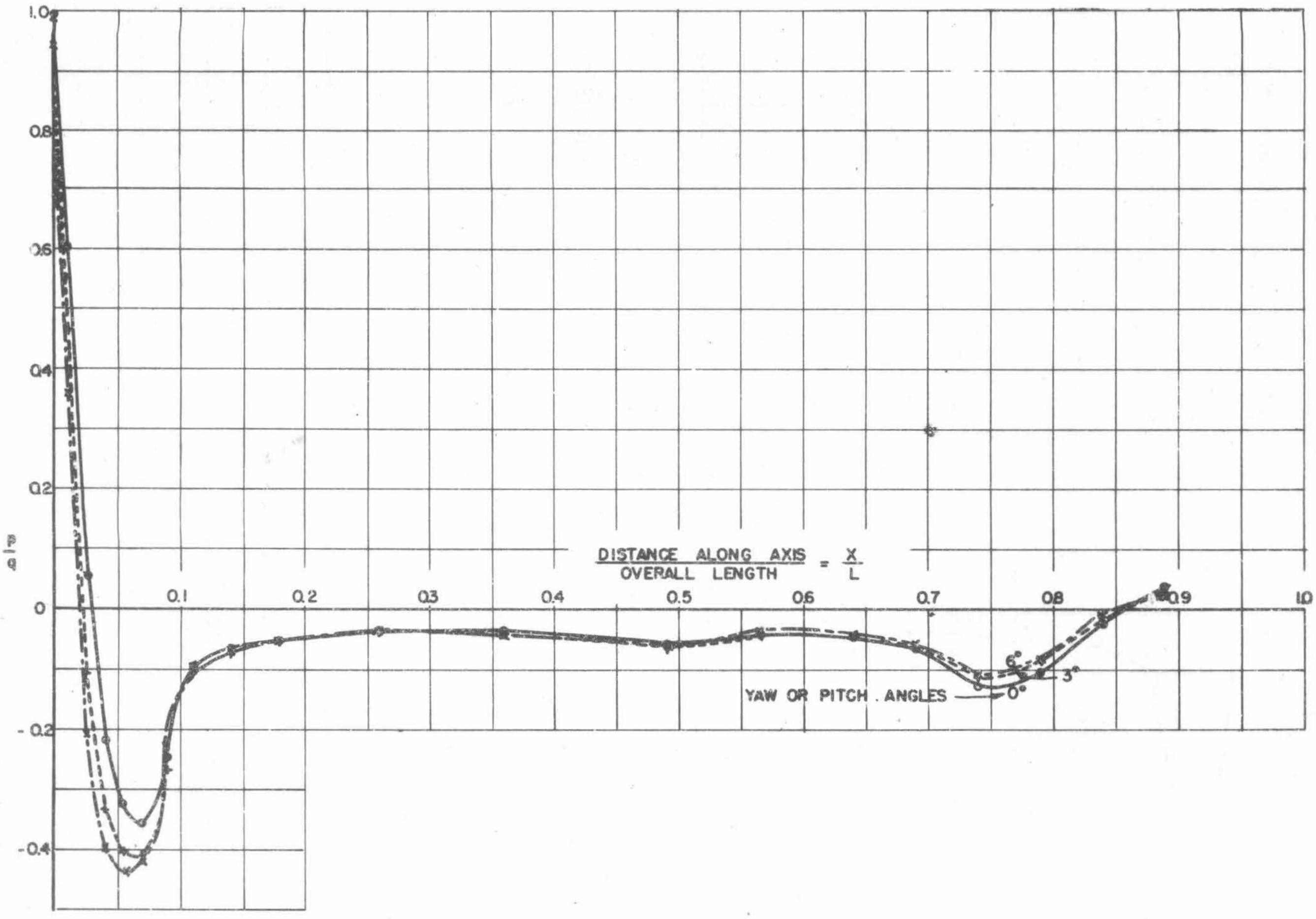

FIG. 23 – MK 14-1 TORPEDO (WITH RING TAIL)

PRESSURE DISTRIBUTION
ALONG LONGITUDINAL SECTION
IN PLANE OF YAW OR PITCH

Lee Side of Body

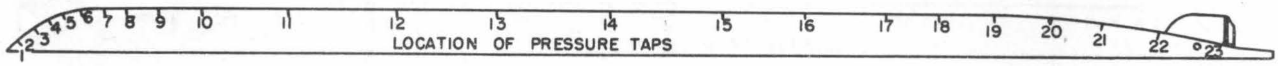

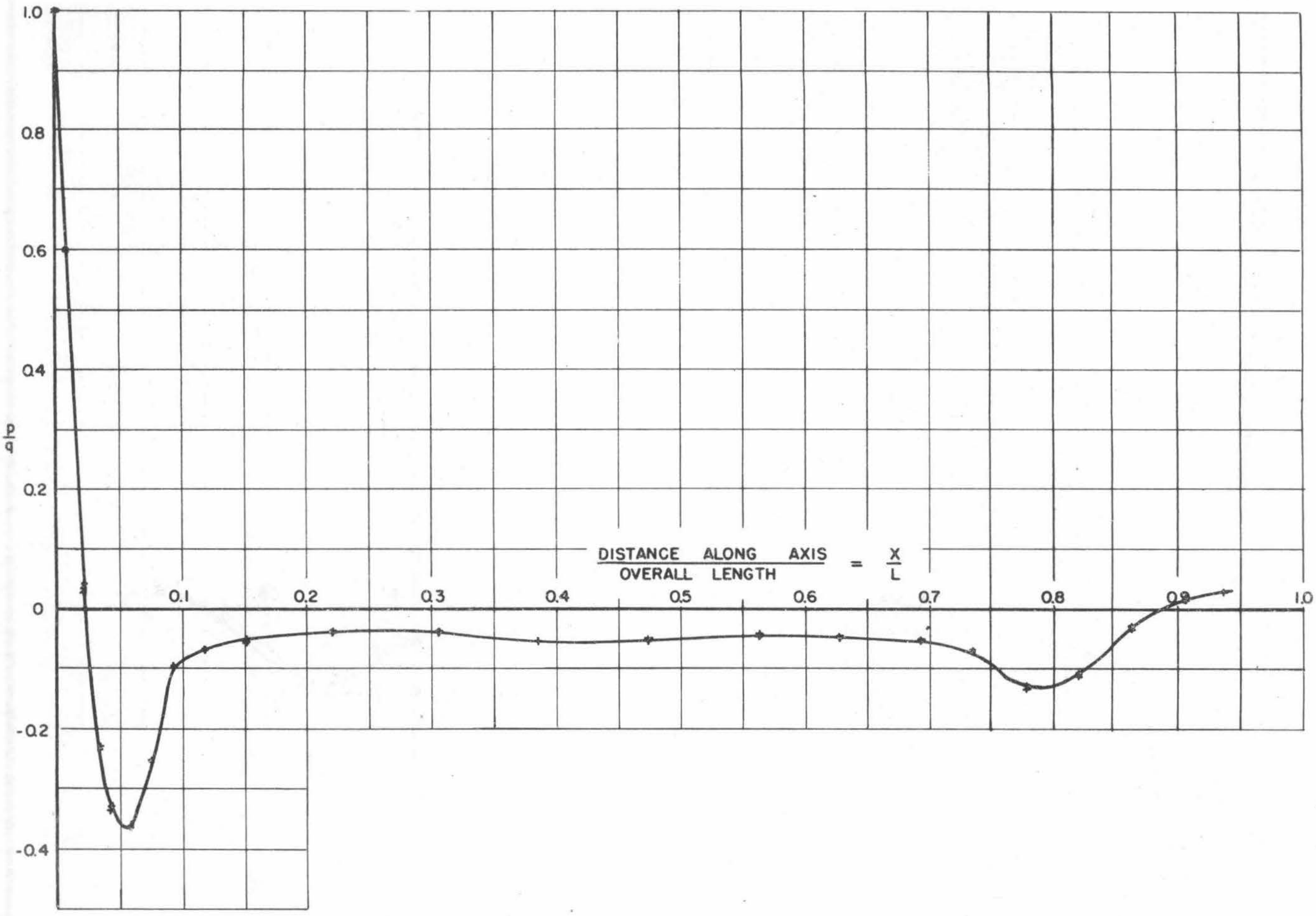

FIG. 24 - MK 15-1 TORPEDO (STANDARD)

PRESSURE DISTRIBUTION
ALONG LONGITUDINAL SECTION

Yaw Angle = 0°

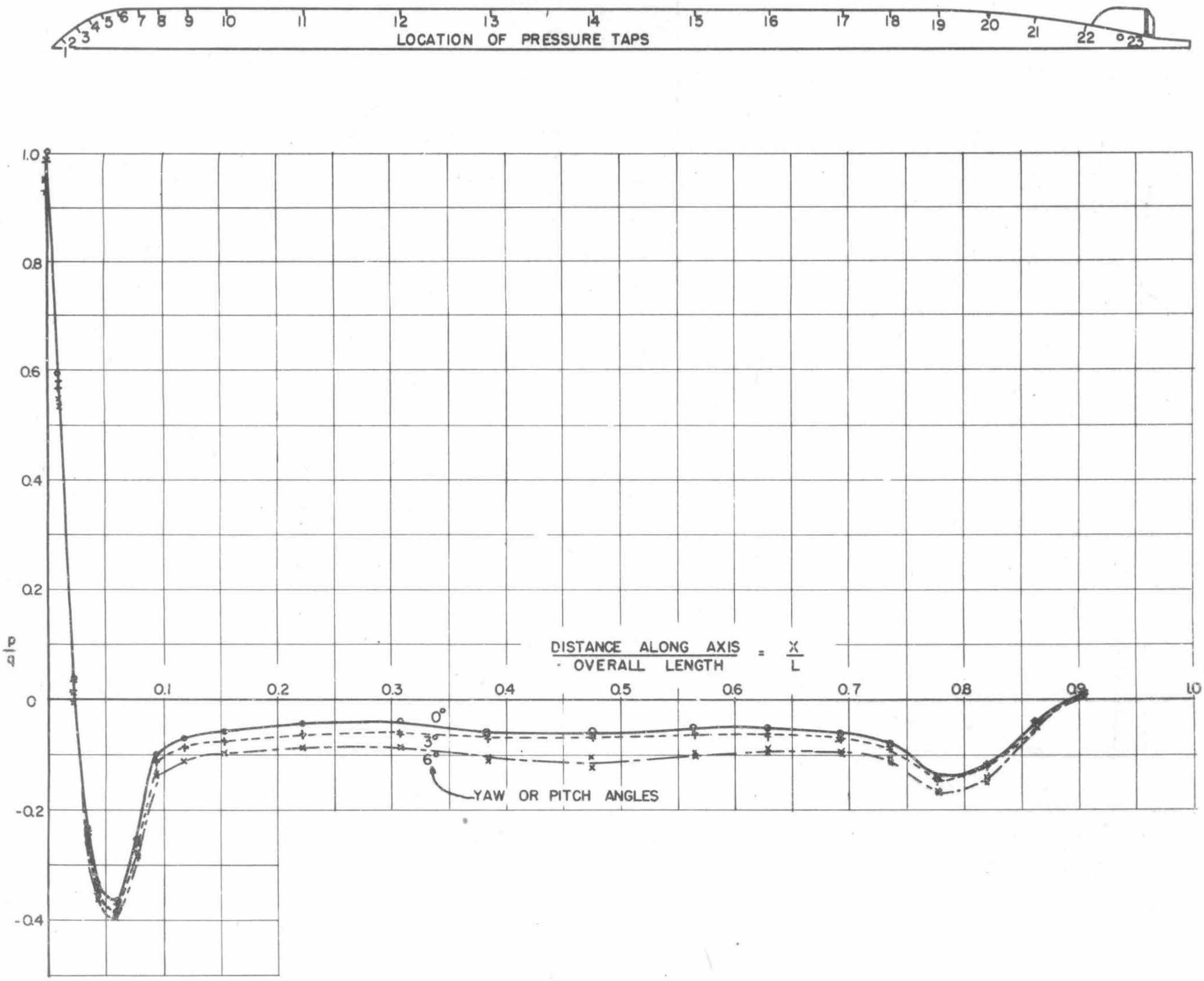

FIG. 25 - MK 15-1 TORPEDO (STANDARD)

PRESSURE DISTRIBUTION
ALONG LONGITUDINAL SECTION
AT RIGHT ANGLES TO PLANE OF YAW OR PITCH

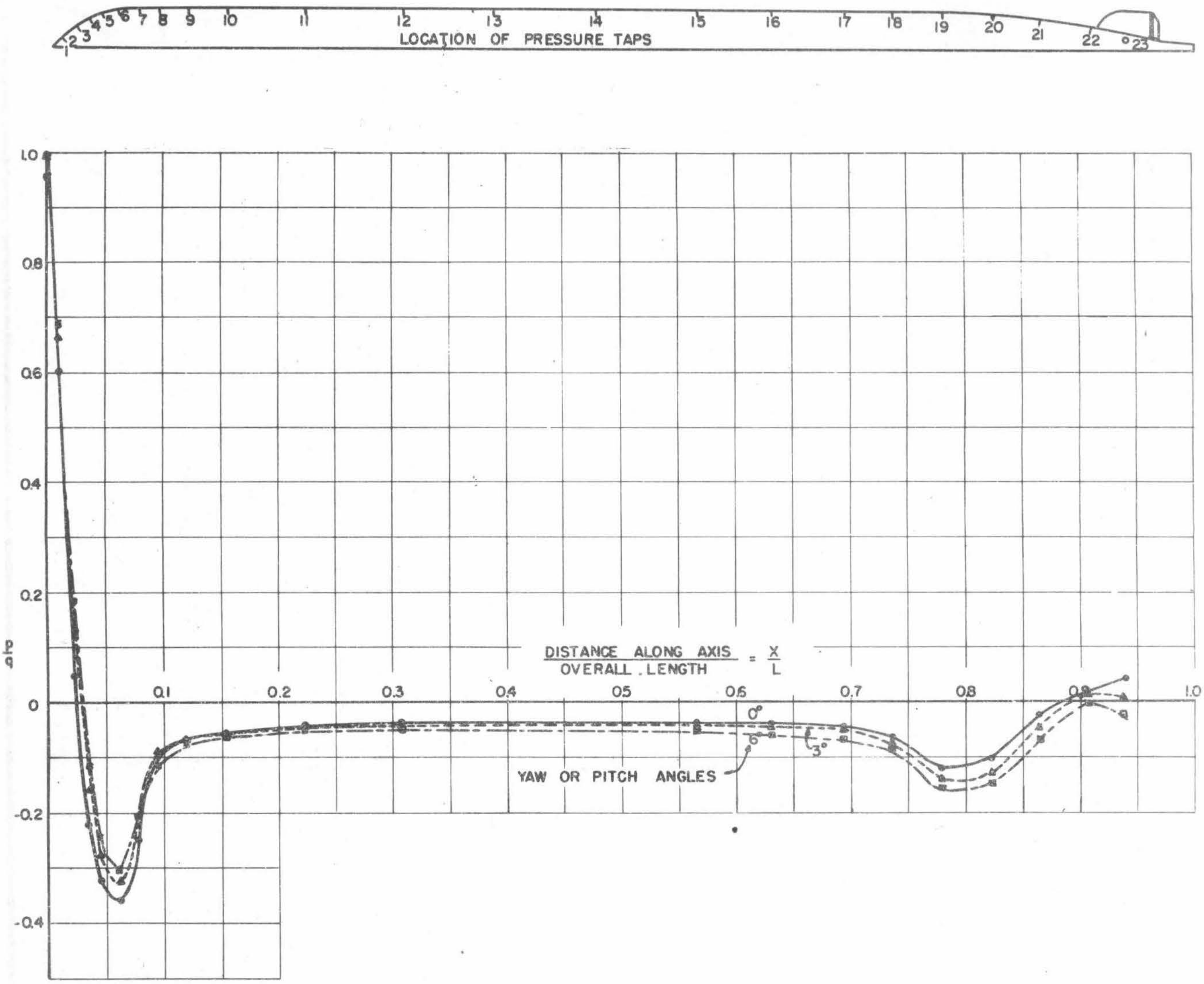

FIG. 26 – MK 15-1 TORPEDO (STANDARD)

PRESSURE DISTRIBUTION
ALONG LONGITUDINAL SECTION
AT 45^{0} TO PLANE OF YAW OR PITCH

Windward Side of Body

CONFIDENTIAL

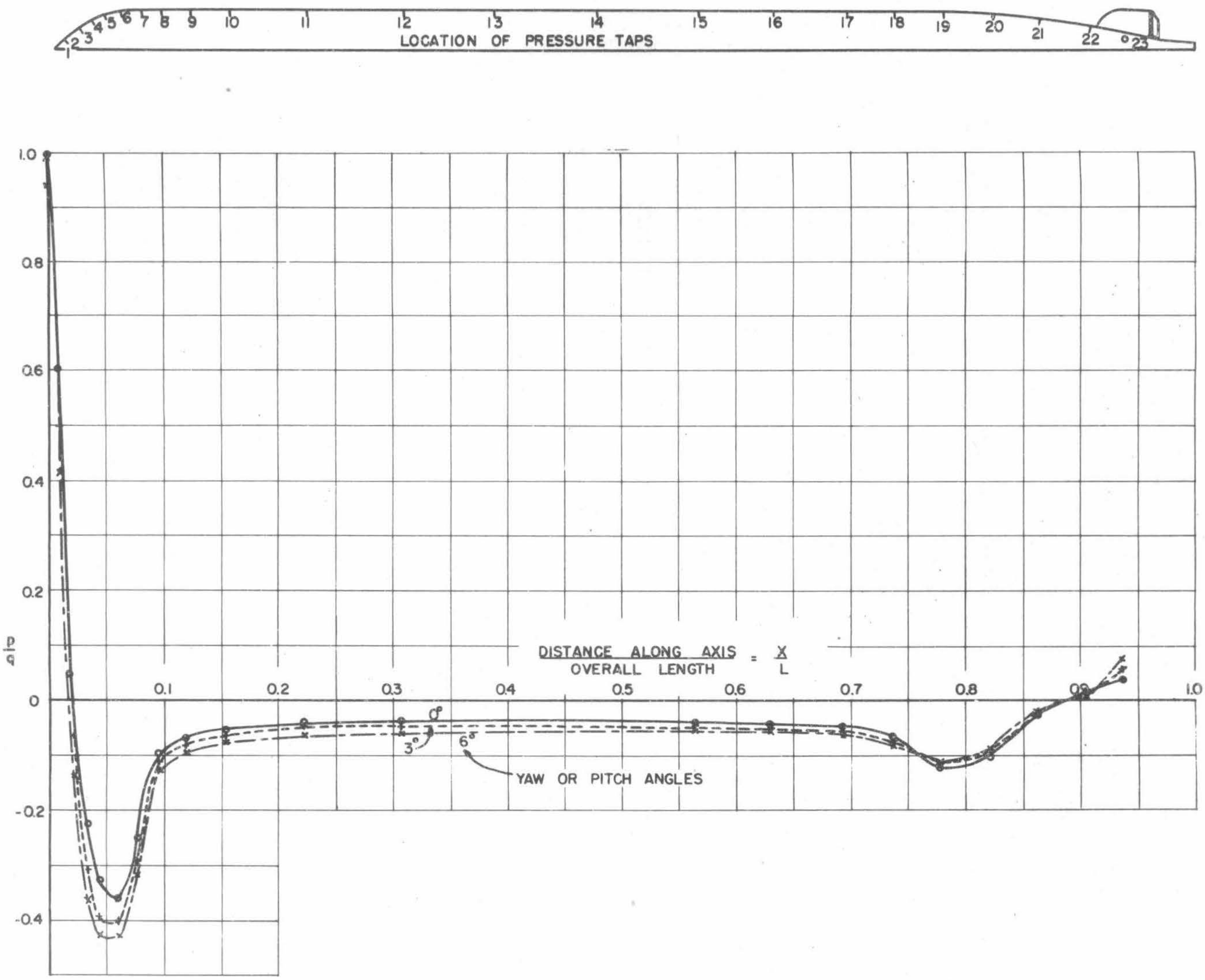

FIG. 27 – MK 15-1 TORPEDO (STANDARD)

PRESSURE DISTRIBUTION
ALONG LONGITUDINAL SECTION
AT 45° TO PLANE OF YAW OR PITCH

Lee Side of Body

CONFIDENTIAL

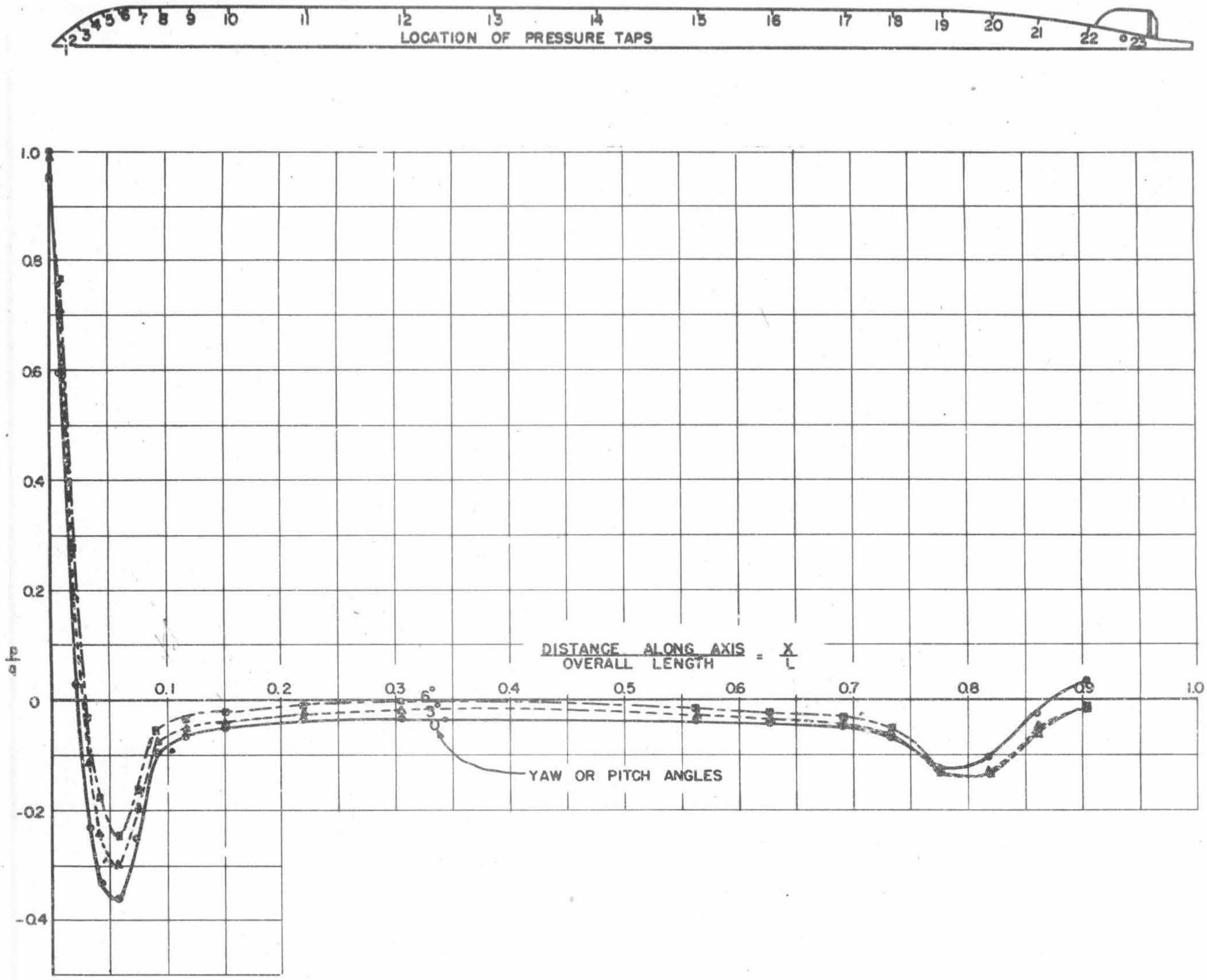

FIG. 28 – MK 15-1 TORPEDO (STANDARD)

PRESSURE DISTRIBUTION
ALONG LONGITUDINAL SECTION
IN PLANE OF YAW OR PITCH

Windward Side of Body

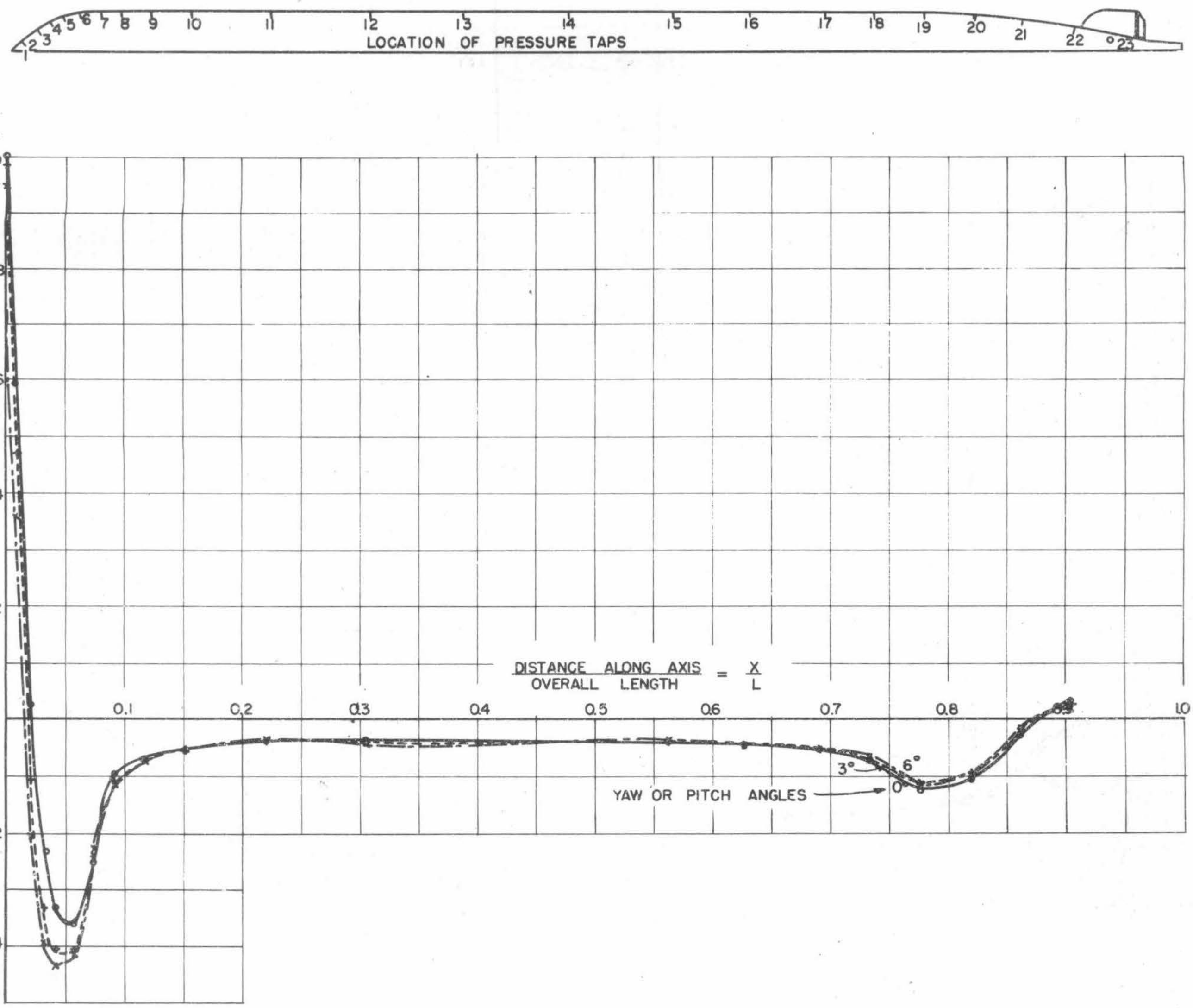

FIG. 29 – MK 15-1 TORPEDO (STANDARD)

PRESSURE DISTRIBUTION
ALONG LONGITUDINAL SECTION
IN PLANE OF YAW OR PITCH

Lee Side of Body

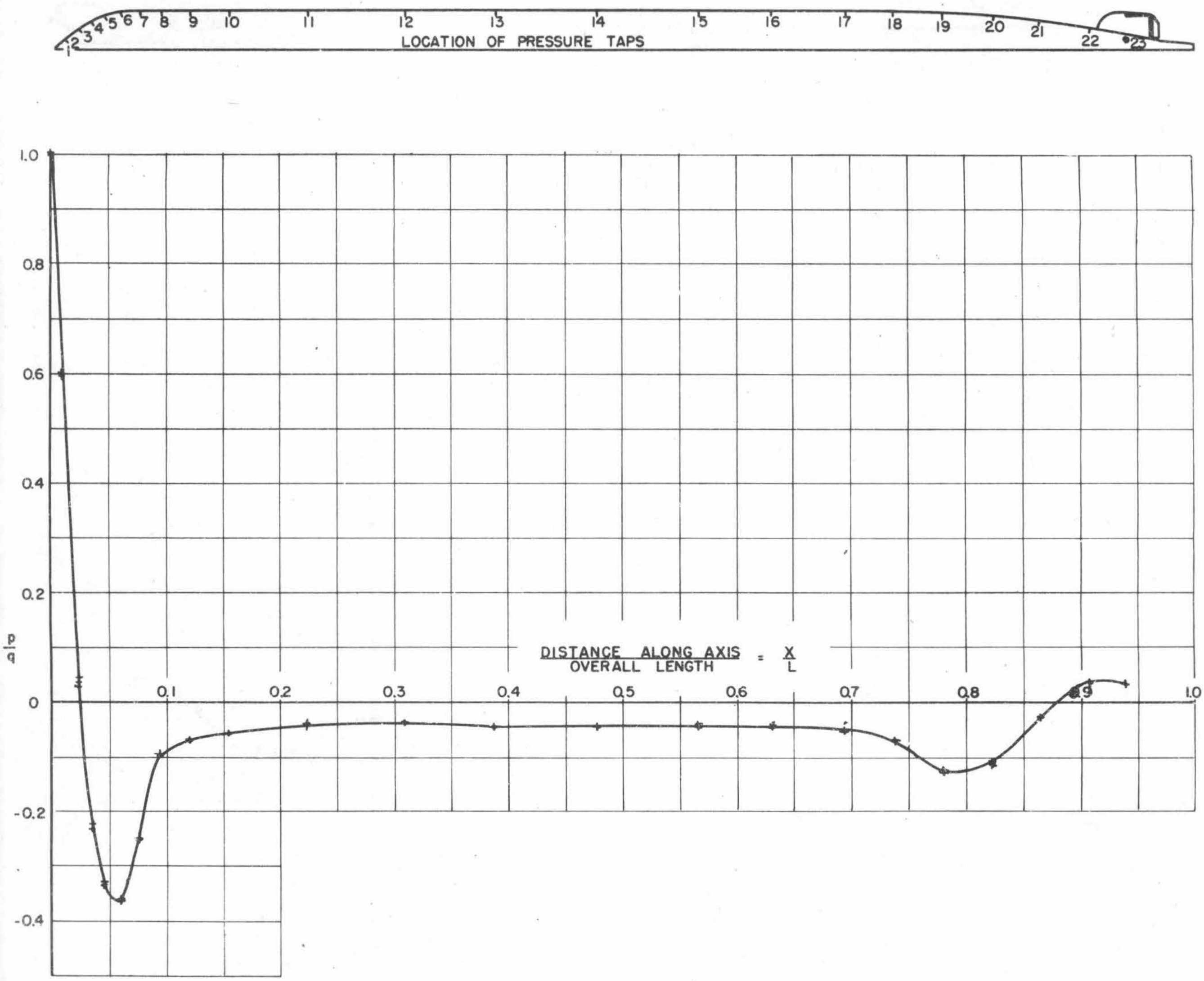

FIG. 30 – MK 15-1 TORPEDO (WITH RING TAIL)

PRESSURE DISTRIBUTION
ALONG LONGITUDINAL SECTION

Yaw Angle = 0°

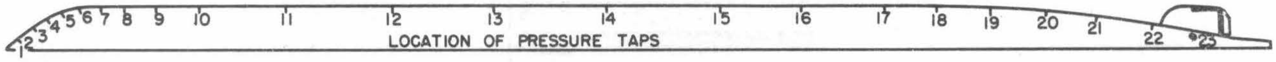

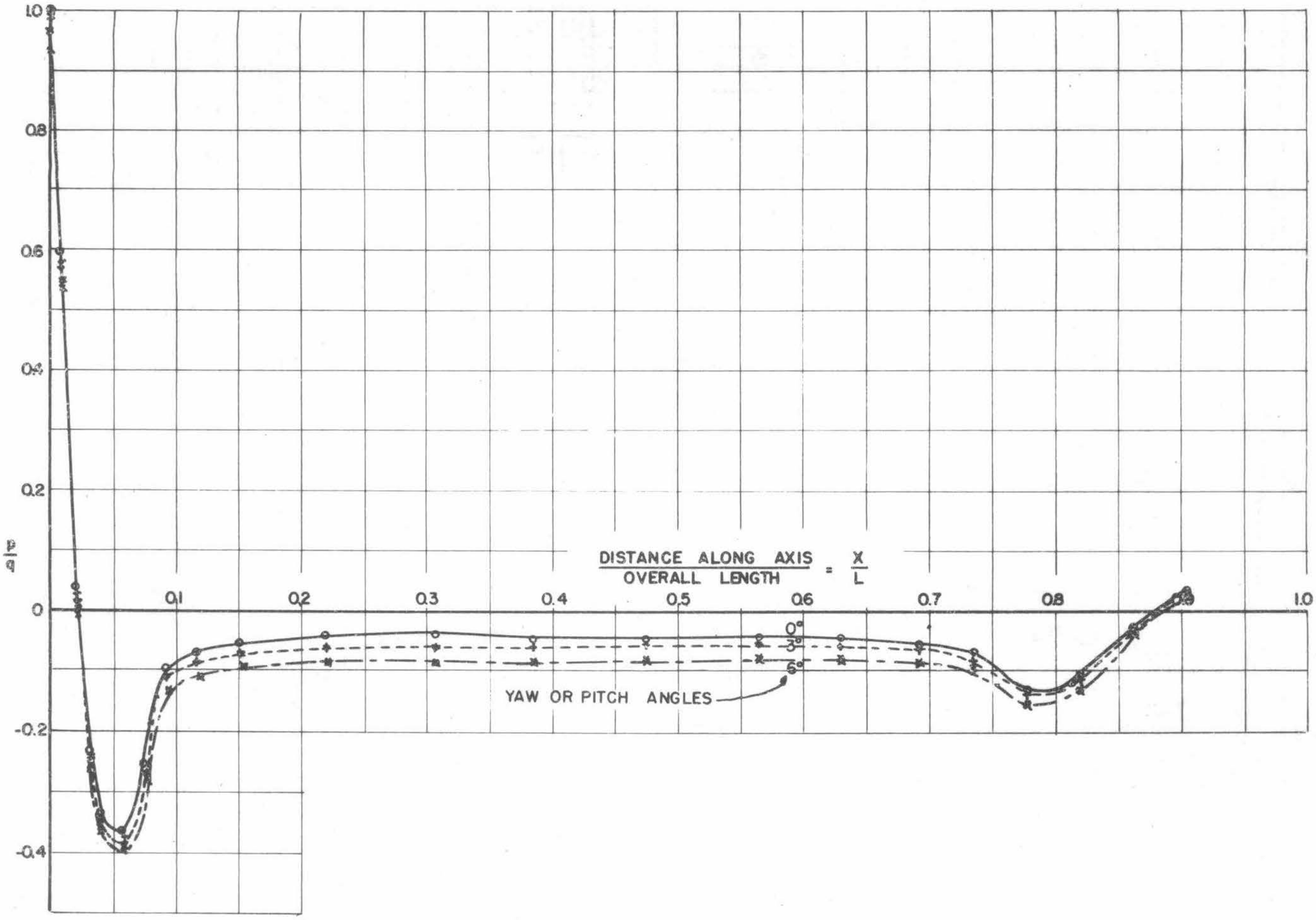

FIG. 31 - MK 15-1 TORPEDO (WITH RING TAIL)

PRESSURE DISTRIBUTION
ALONG LONGITUDINAL SECTION
AT RIGHT ANGLES TO PLANE OF YAW OR PITCH

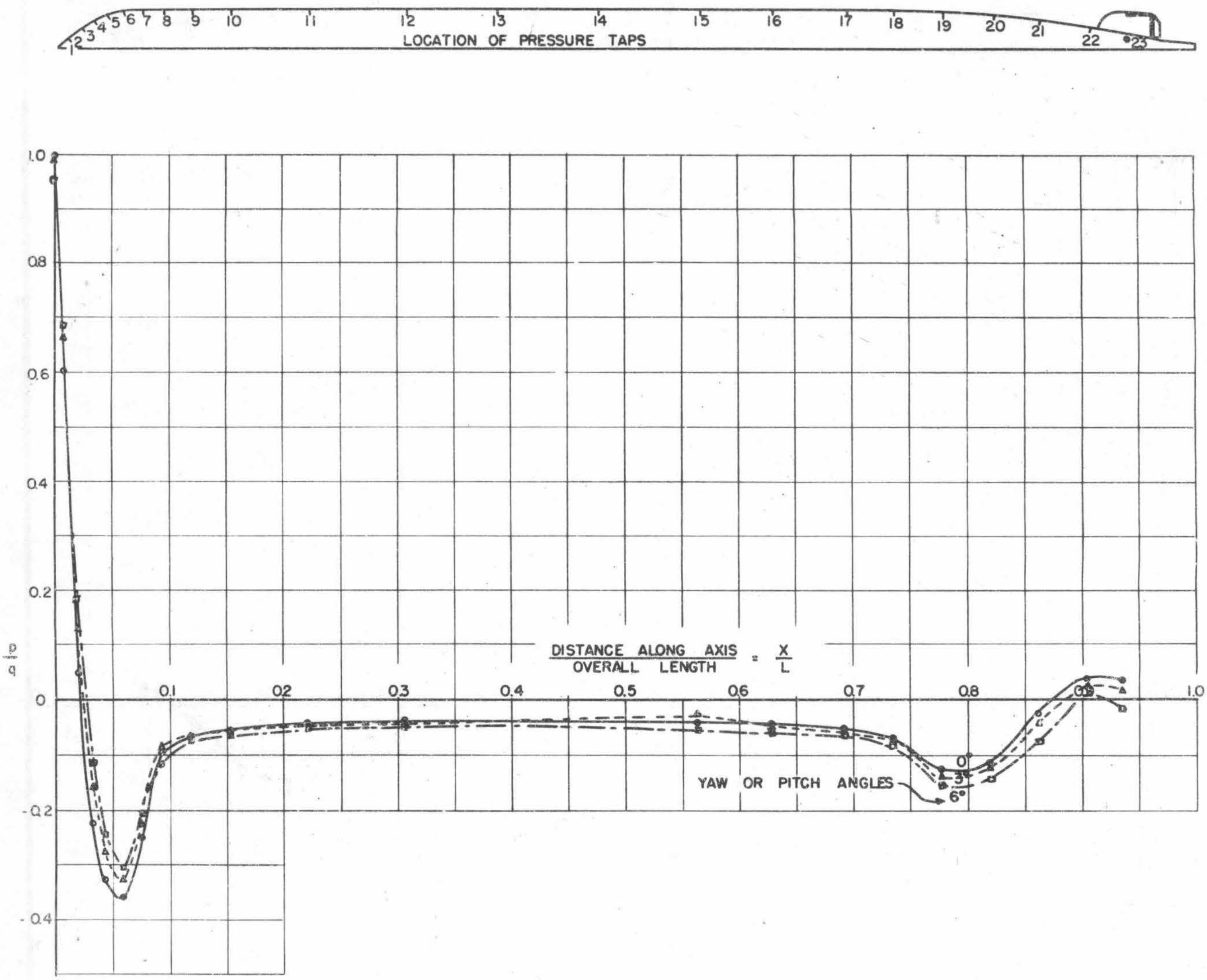

FIG. 32 – MK 15-1 TORPEDO (WITH RING TAIL)

PRESSURE DISTRIBUTION
ALONG LONGITUDINAL SECTION
AT 45° TO PLANE OF YAW OR PITCH

Windward Side of Body

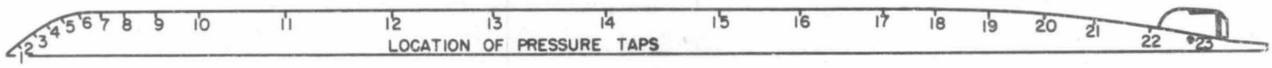

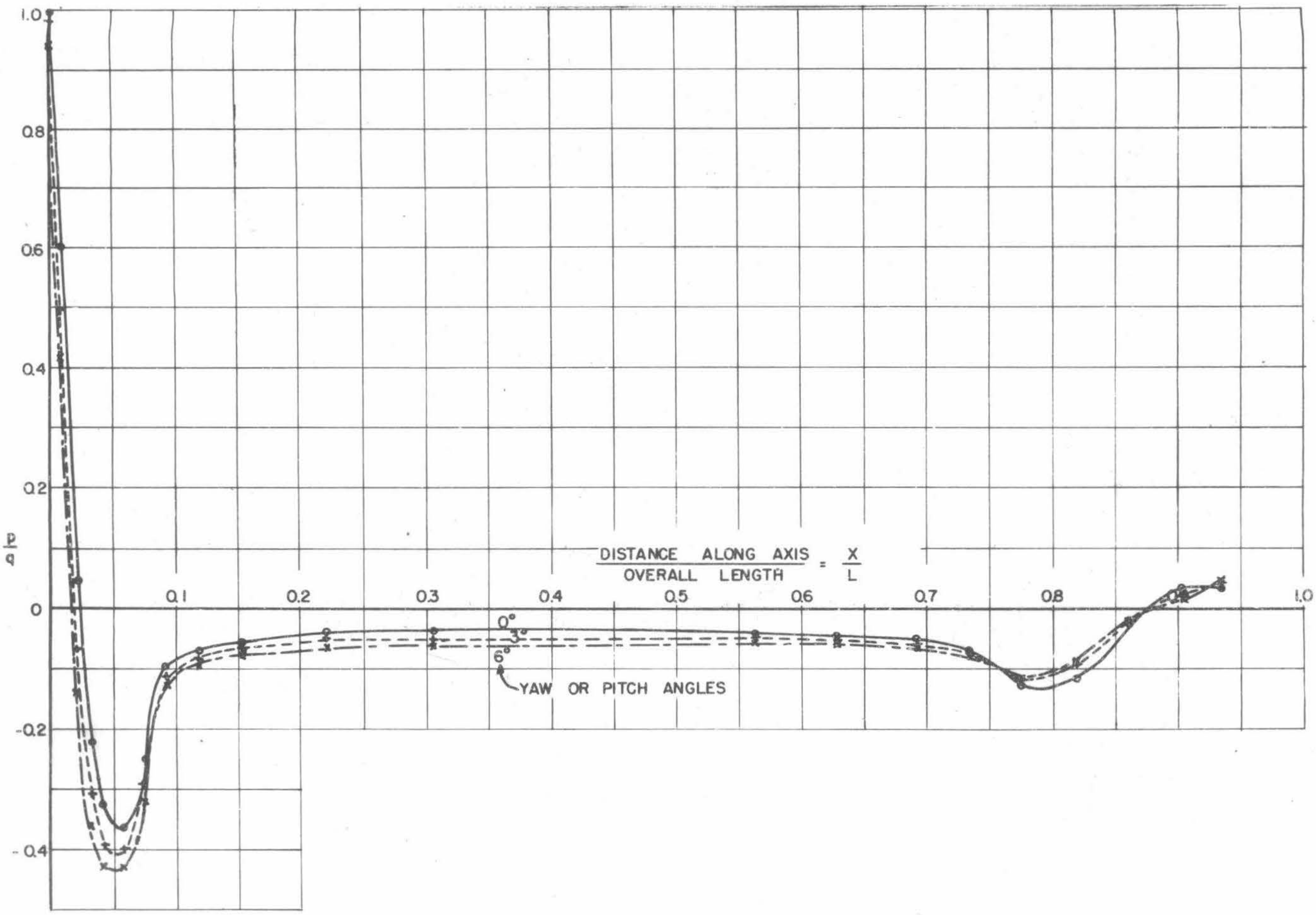

FIG. 33 - MK 15-1 TORPEDO (WITH RING TAIL)

PRESSURE DISTRIBUTION
ALONG LONGITUDINAL SECTION
AT 45° TO PLANE OF YAW OR PITCH

Lee Side of Body

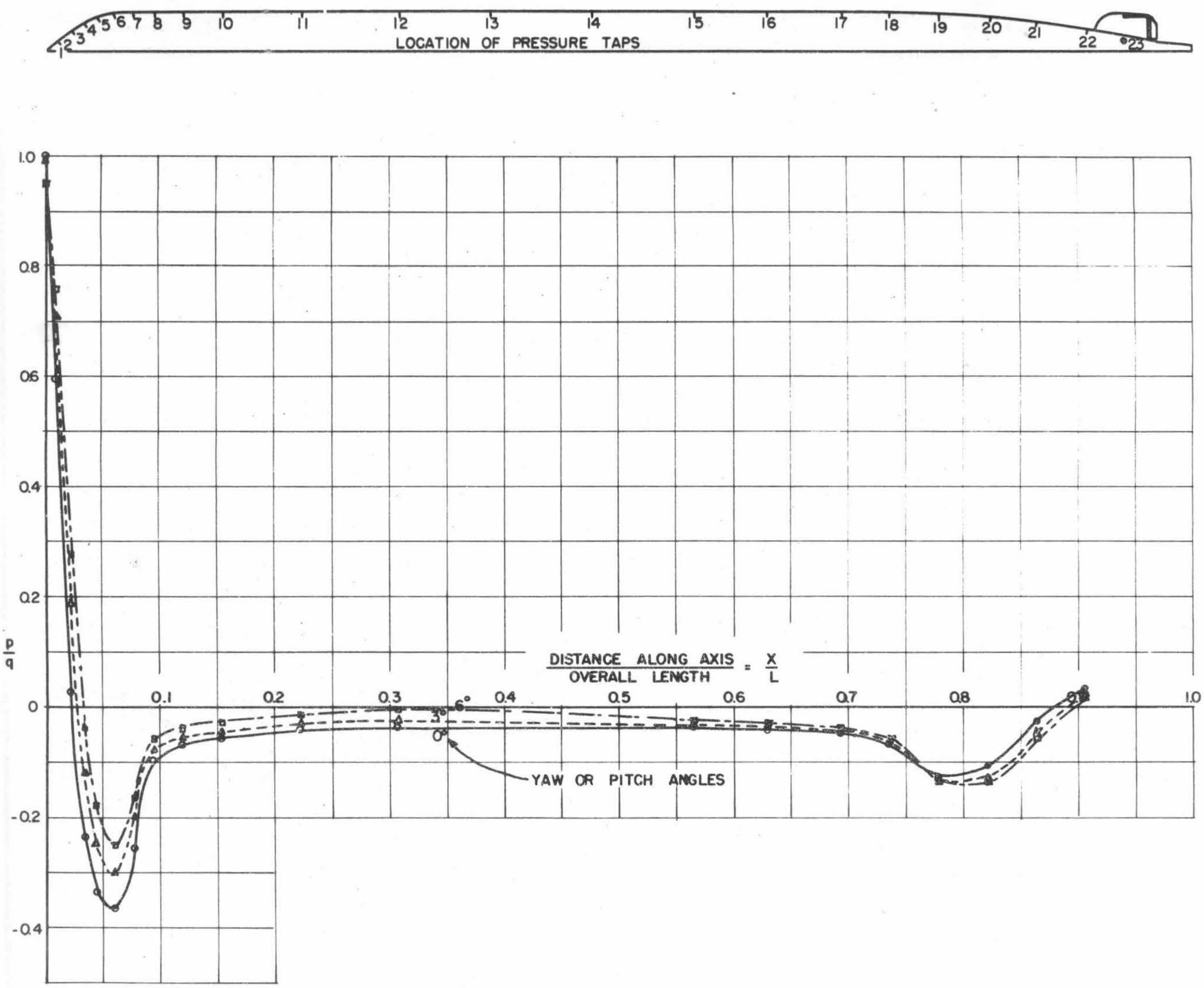

FIG. 34 - MK 15-1 TORPEDO (WITH RING TAIL)

PRESSURE DISTRIBUTION
ALONG LONGITUDINAL SECTION
IN PLANE OF YAW OR PITCH

Windward Side of Body

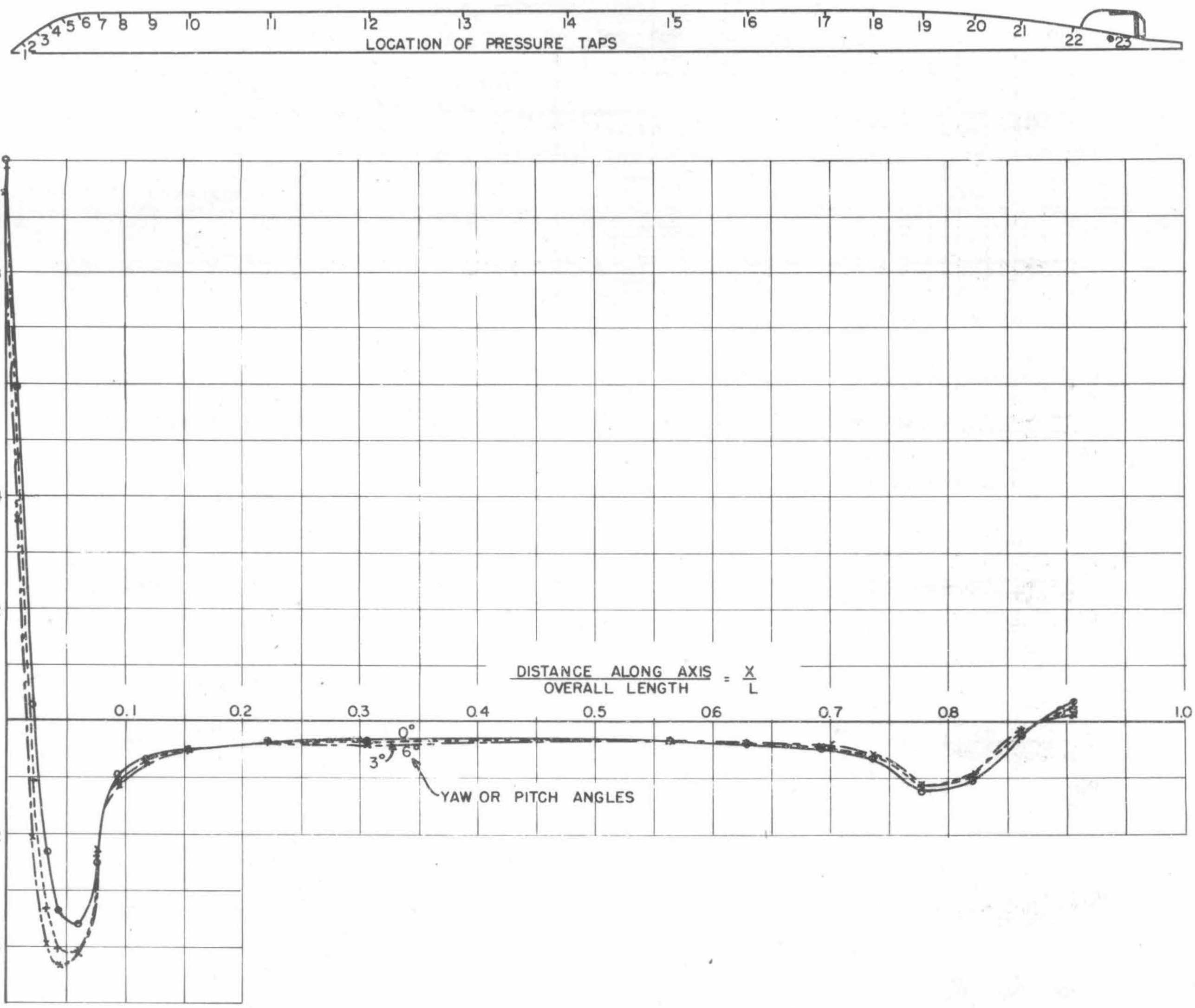

FIG. 35 – MK 15-1 TORPEDO (WITH RING TAIL)

PRESSURE DISTRIBUTION
ALONG LONGITUDINAL SECTION
IN PLANE OF YAW OR PITCH

Lee Side of Body

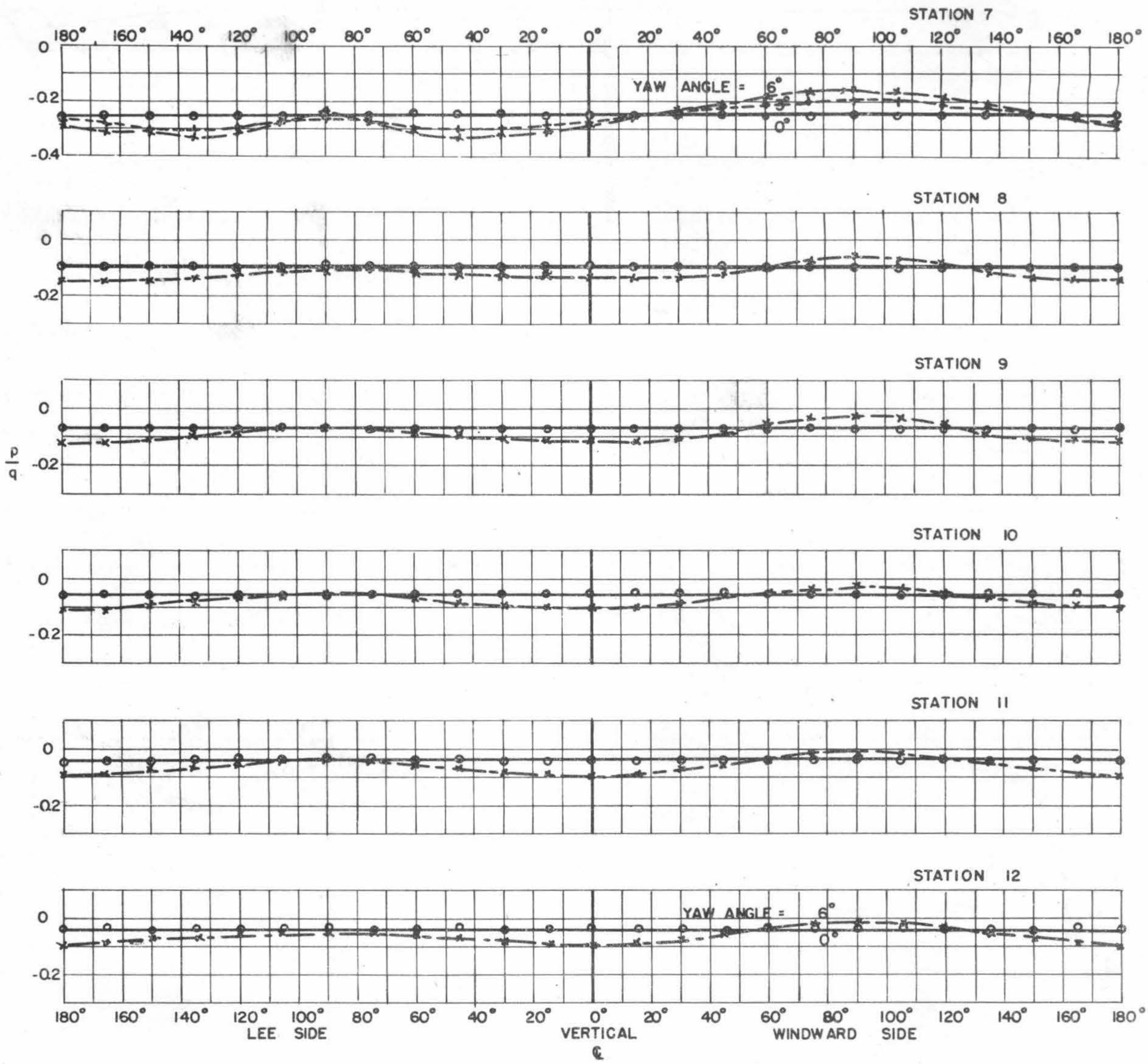

FIG. 36– MK 14-1 TORPEDO

PRESSURE DISTRIBUTION
ABOUT NORMAL CROSS SECTIONS
AT STATIONS ON FOREBODY

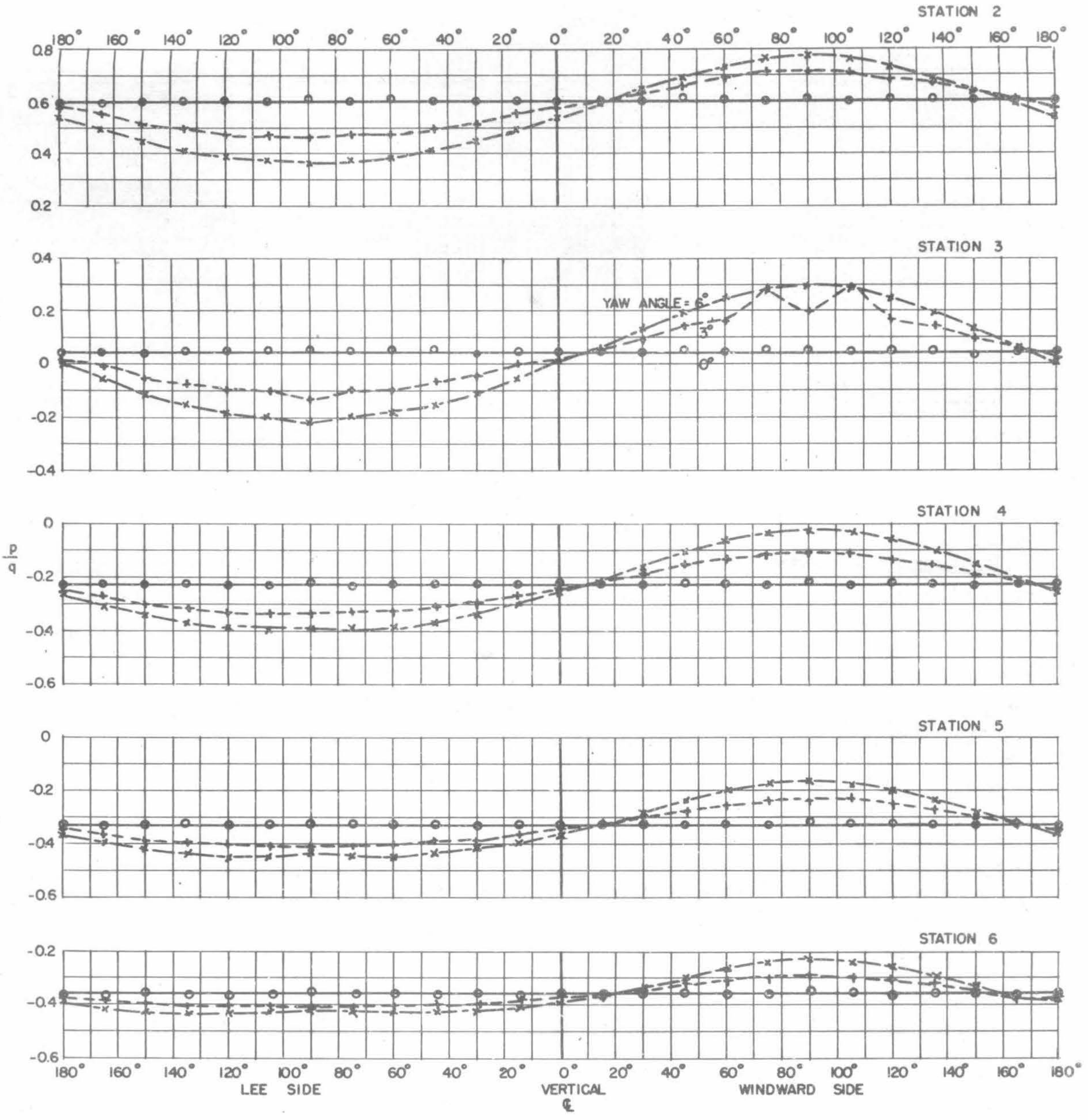

FIG. 37 - MK 14-1 TORPEDO

PRESSURE DISTRIBUTION
ABOUT NORMAL CROSS SECTIONS
AT STATIONS ON FOREBODY

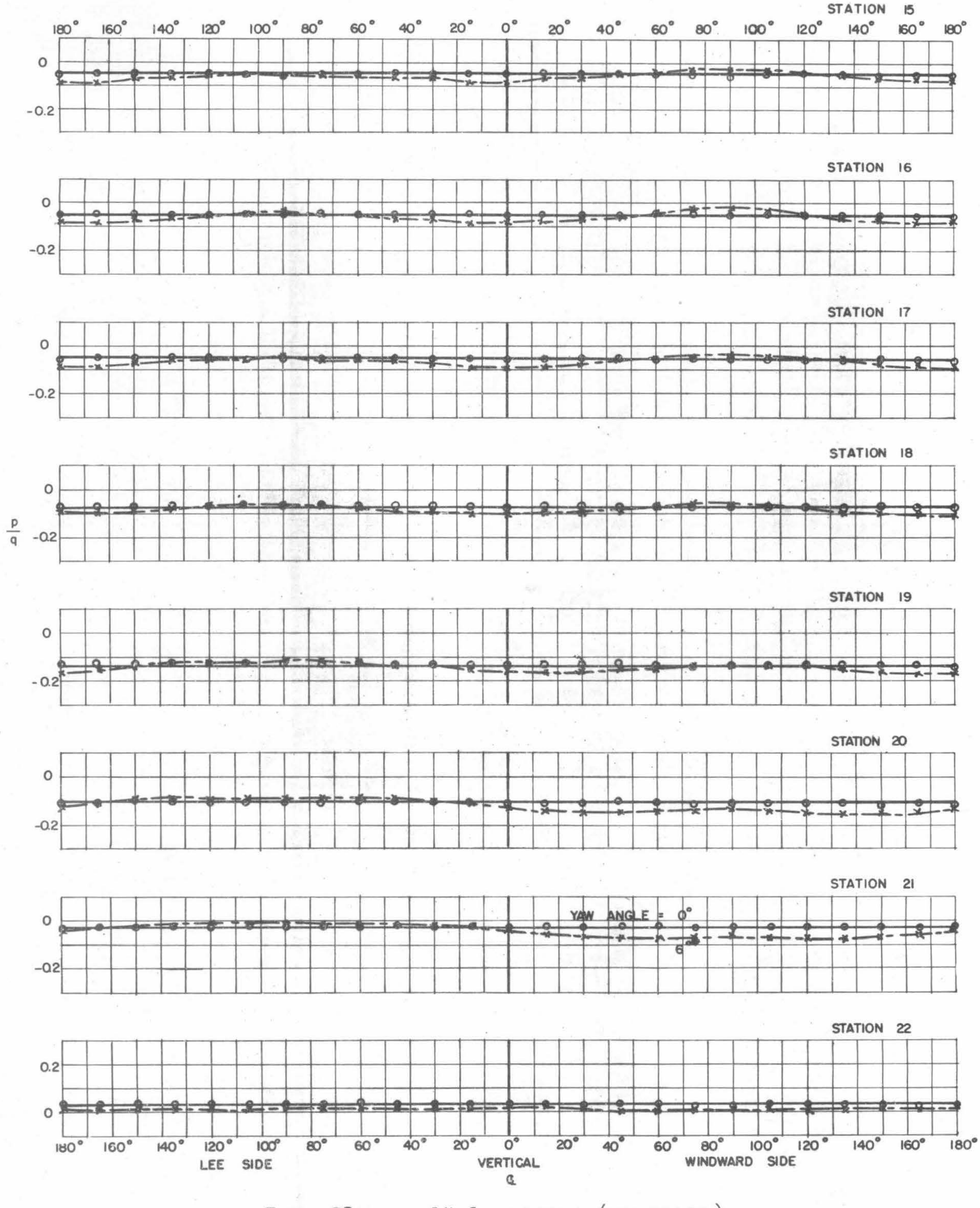

FIG. 38 - MK 14-1 TORPEDO (STANDARD)

PRESSURE DISTRIBUTION
ABOUT NORMAL CROSS SECTIONS
AT STATIONS ON AFTERBODY

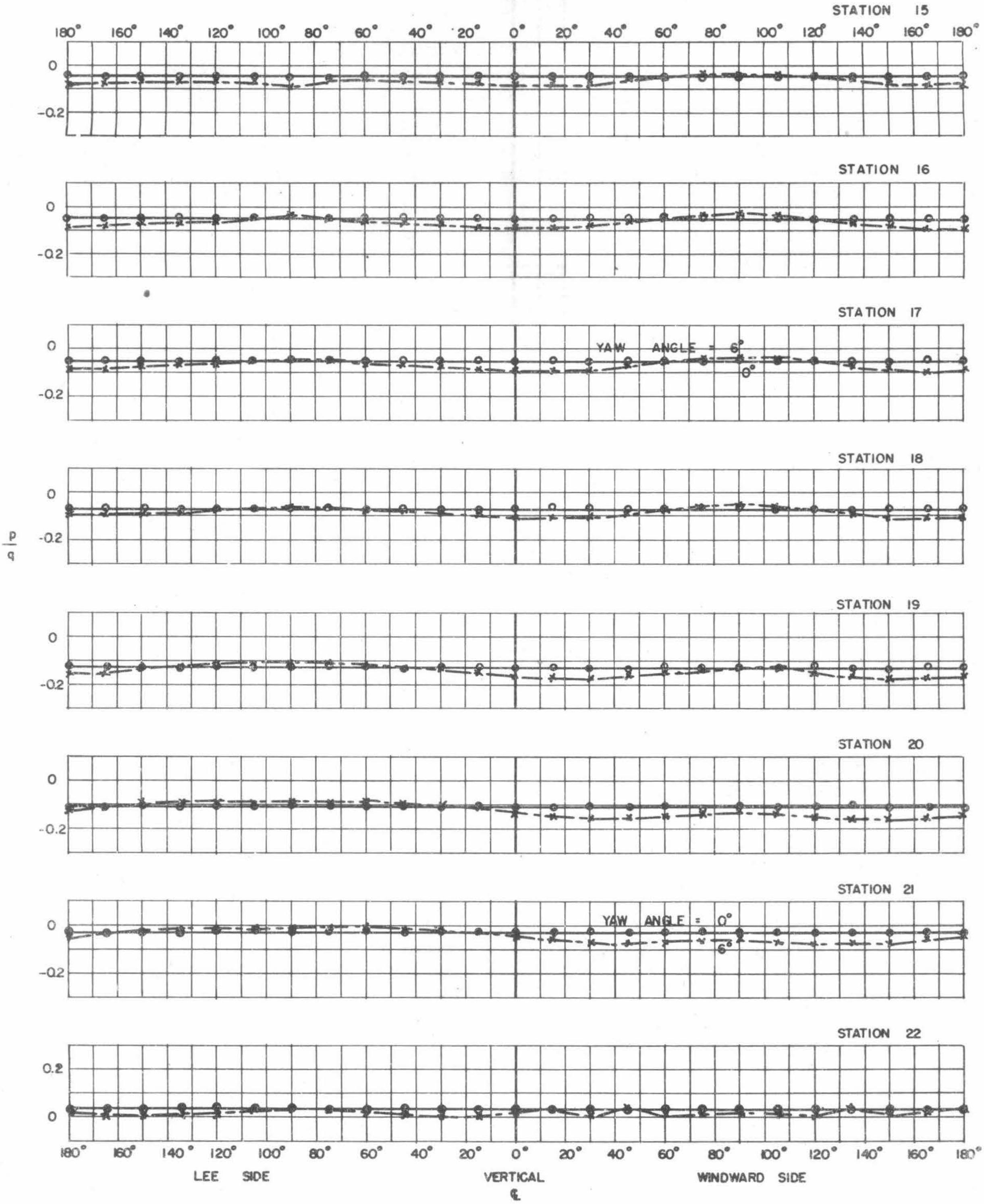

FIG. 39 — MK 14-1 TORPEDO (WITH RING TAIL)

PRESSURE DISTRIBUTION
ABOUT NORMAL CROSS SECTIONS
AT STATIONS ON AFTERBODY

CAVITATION AND PRESSURE DISTRIBUTION

Cavitation, or the formation of vapor-filled cavities, occurs in hydraulic machinery or on underwater projectiles when the pressure at any point on the body becomes equal to the vapor pressure of the water. A knowledge of the pressure distribution around a projectile should, therefore, give an indication of the susceptibility of the projectile to cavitate. As defined in the preceding section, the data presented herein are given in terms of

$$\left(\frac{p}{q}\right) = \frac{P - P_o}{1/2\rho V^2}$$

In order to have cavitation, the pressure on the body, P, must equal the vapor pressure P_v, or

$$P_v = P = \left(\frac{p}{q}\right) 1/2 \, \rho \, V^2 + P_o$$

From the above equation it is evident that cavitation cannot occur on the body at a point having a positive value of (p/q), for then the static pressure P_o must be lower than P_v, and the entire volume of the liquid would boil. With a negative (p/q), it is seen that, for a given water temperature (i.e., given P_v), cavitation conditions are approached as P_o is lowered or as V is increased. As cavitation is brought about, it will begin at that point on the body having the lowest value of (p/q). Thus, the lowest value of (p/q) measured on the body is an index of its susceptibility to cavitation, and is normally given as the cavitation parameter, K, which is defined by

$$K = \frac{P_o - P_v}{1/2 \, \rho \, V^2}$$

Comparing this equation with the expression for (p/q), it is seen that $K = -(p/q)_{min}$, i.e., the cavitation parameter for the inception of cavitation on any shape is equal, but of opposite sign, to the lowest value of (p/q) measured on that body.

The curves of Figures 12, 18, 24, and 30, indicate, therefore that the inception of cavitation on these torpedoes should occur at a K value of about 0.36, which is in good agreement with the value of 0.34 reported in Reference 1 from direct observation of cavitation.

As the value of K is lowered further, the zone of cavitation grows and the pressure distribution is modified, because the water now flows around the vapor pocket as well as around the body. Nevertheless, from Figures 12, 18, 24, and 30 it could be predicted that as K is lowered a point would be reached where the pressure on the body at the second minimum pressure point (on the afterbody) would become equal to the vapor pressure of the water, and a second zone of cavitation would develop there.

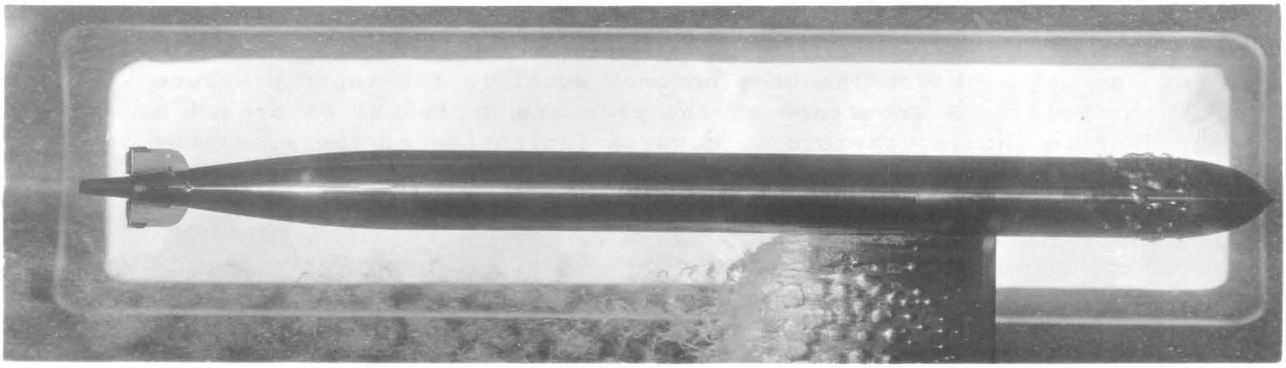

FIG. 40 - CAVITATION ON MODEL OF MK 14-1
K = 0.25

FIG. 41 - CAVITATION ON MODEL OF MK 14-1
K = 0.15

The photograph of Figure 40 was used in Reference 1 to illustrate an early stage of cavitation, some time after inception, at a K value of 0.25. It is seen that the cavitation occurs approximately in the zone where the value of p/q is lower than 0.25. As the bubbles are carried downstream into a region of higher pressure, they collapse and disappear. Figure 41 shows a more advanced stage of cavitation, at a K value of 0.15, with a second well developed zone of cavitation originating on the afterbody.

PRESSURE INTAKES FOR DEPTH CONTROL AND DEPTH AND ROLL RECORDER

DEPTH CONTROL

To enable a multi-speed torpedo to travel at set depth under all conditions of speed and orientation with the direction of travel, it is necessary that the pressure impressed upon the hydrostatic diaphragm of the depth-control mechanism be at all times equal to the static pressure of the water at the actual running depth of the torpedo. This is best accomplished by locating the pressure intake to the hydrostat at a point on the body where the pressure at the surface, under all conditions of speed, yaw and pitch, is equal to the static pressure in undisturbed water, that is, at a point where p/q is equal to zero at all yaw or pitch angles. Also, the intake opening should be flush with the surface, at right angles to it, and with smooth edges.

Examination of Figures 12 and 18 shows that, on the Mk 14-1 afterbody, $p/q = 0$ where $X/L = 0.855$, or at a distance of about 35 inches from the tail end, slightly aft of piezometer Tap No 21 (see also Figure 11). The same location also holds for the Mk 15-1. On the MK 15-1 curves, because of the greater length of this torpedo, this is at $X/L = 0.875$. Inspection of the transverse pressure distribution about Station 21 (Figures 38 and 39), shows that with zero yaw the value of p/q at this station is just barely lower than zero, and that it varies but slightly with yaw, rising on the lee side and dropping on the windward side. The best arrangement for the pressure intake would be, therefore, through a piezometer ring connecting four small openings uniformly distributed about the circumference of the torpedo and 35 inches ahead of the end of the tail. With this arrangement, the slight yaw effect would be averaged out.

With the pressure intake at any other location on the afterbody, it is evident from the pressure distribution curves that the pressure at the surface would, for a given yaw angle, differ from true static pressure by a fixed fraction of the velocity head. For a single-speed torpedo the pressure impressed on the diaphragm would differ from static pressure by a constant number of feet, and this can be taken into account in the calibration of the depth setting mechanism. In a multi-speed torpedo, this method of correction would require a different calibration at each speed. Another method of correcting for mislocation of the pressure intake is to so design the intake that the pressure transmitted to the diaphragm differs from the normal pressure at the surface by the required fraction of the velocity head. This can be done by drilling the pressure taps at some angle other than normal to the surface, or by using scoops or baffles. These methods, however, are likely to be highly sensitive to changes in yaw or pitch. It is evident, therefore, that if the present arrangement of the pressure intake is unsatisfactory, the best solution would be the one recommended above, that is, with smooth-edged piezometer openings drilled at right angles to the surface and located where p/q = O. The experience of this laboratory indicates that piezometer openings with slightly rounded edges (to a radius of about 1/6 the bore diameter) are more accurate and reliable than sharp-edged openings.

INFLUENCE OF PROPELLERS

It should be noted that the tests reported herein were made on a model without propellers. The operation of the propellers on the prototype torpedoes may modify the pressure distribution on the afterbody, so that the best location for the pressure intake may be slightly ahead or aft of the position indicated above.

DEPTH AND ROLL RECORDER

The requirements discussed in the preceding paragraphs in connection with the location and design of the pressure intake for the depth control mechanism apply also to the pressure intake for the hydrostatic diaphragm of the depth and roll recorder, if the instrument is to record true running depth. Since this instrument is installed in the head, it would not be practicable to connect it to the point on the afterbody where p/q = O. Connection to the point on the nose where p/q = O is not recommended because at this point the pressure varies greatly with yaw or pitch. If the depth and roll recorder does not record true depth, it would probably be best to determine the magnitude of the error and apply a correction.

It should be borne in mind that the depth control mechanism and the depth and roll recorder should not be used as primary instruments to check each other, because it is possible to have the torpedo run above or below set depth and at the same time to get a depth record which indicates a run at set depth. The pressure distribution curves show that the pressure over most of the surface of the torpedo is lower than static pressure. It is possible, therefore, that the pressures impressed on both depth control and depth and roll recorder diaphragms are lower than static pressure. In this case, the torpedo would run below set depth but the depth and roll recorder would indicate a depth shallower than the actual running depth, and thus the error may not be detected.